

Supporting Information

Conformer-Specific [1,2]H-Tunnelling in Captodatively-Stabilized Cyanohydroxycarbene ($\text{NC}-\ddot{\text{C}}-\text{OH}$)

André K. Eckhardt, Frederik R. Erb, and Peter R. Schreiner*

Institute of Organic Chemistry, Justus Liebig University, Heinrich-Buff-Ring 17, 35392 Giessen (Germany); prs@uni-giessen.de

Table of Contents

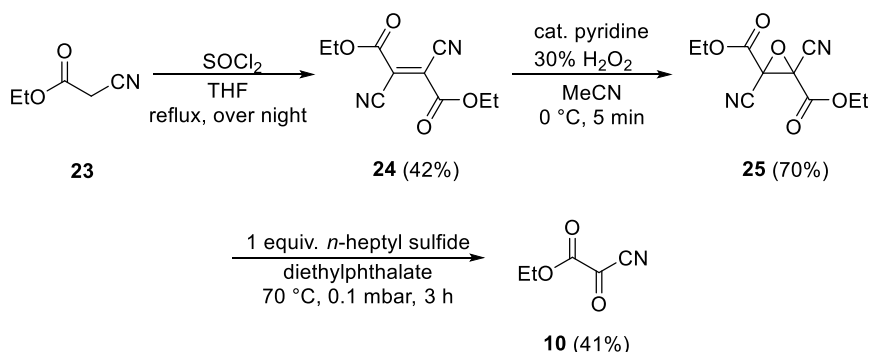
Methods	S2
NMR Spectra.....	S6
Matrix Isolation Infrared Spectra	S14
Matrix Isolation UV/Vis Spectrum	S21
Spectroscopic Data	S22
Tunnelling Kinetic Analysis.....	S25
WKB Tunnelling Computations.....	S27
Polyrate Tunnelling Computations.....	S29
Instanton Tunnelling Computations	S31
NBO Analysis.....	S32
Potential Energy Surfaces and Cartesian Coordinates for Selected Structures	S35
References and Full Citations for Electronic Structure Codes	S47

Methods

Matrix isolation studies. For all matrix isolation studies a Sumitomo cryostat system consisting of an F-70 compressor unit and an RDK 408D2 closed-cycle refrigerator was used. The vacuum shroud surrounding the coldhead was outfitted with polished KBr windows for IR and BaF₂ windows for UV/Vis measurements, whereas the coldhead was equipped with a CsI window for IR and a BaF₂ window for UV/Vis measurements, respectively. Spectra were recorded with a Bruker Vertex 70 FT IR spectrometer ($4500 - 400\text{ cm}^{-1}$, resolution 0.7 cm^{-1}), while UV/Vis spectra were recorded with a JASCO V-670 spectrophotometer. For a single measurement, a total of 50 scans was accumulated. The temperature of the cold window was measured with a Si-diode connected to a Lakeshore 336 temperature controller. For the combination of high-vacuum flash pyrolysis with matrix isolation, we employed a small, home-built, water-cooled oven, which was directly connected to the vacuum shroud of the cryostat. The pyrolysis zone consisted of an empty quartz tube with an inner diameter of 8 mm, which was resistively heated over a length of 50 mm by a coaxial wire. The temperature was monitored with a NiCr–Ni thermocouple. In a typical pyrolysis experiment ethyl 2-cyano-2-oxoacetate **10** was evaporated from a pre-cooled ($-45\text{ }^{\circ}\text{C}$) storage vessel connected directly with the quartz pyrolysis tube at temperatures of $900\text{ }^{\circ}\text{C}$. The matrix gas argon was added via a separate jet in very high excess to achieve the desired spatial separation of pyrolysis product in the thus formed argon matrix. An exact dopant/argon ratio cannot be given using this procedure, but the dopant/argon ratio is estimated to be ca. 1:500. The gas flow was regulated by a Pfeiffer EVN 116 gas dosing valve with separate shut-off. For all experiments we used Ar of 99.999% purity. Narrow-band NIR irradiation was performed with an optical parametric oscillator (GWU OPO versaScan 280 MB, pump laser: Spectra-Physics Quanta Ray Nd:YAG LAB-170-10, 355 nm, line width 4 cm^{-1}). Irradiation with green light (520 nm) was performed with a commercially available LED.

Computations. All coupled cluster computations were carried out with the CFOUR program package. In general, the all electron coupled cluster level of theory¹⁴ including single, double, and perturbatively included triple excitations [AE-CCSD(T)] utilizing the Dunning correlation consistent split valence basis set cc-pCVQZ⁵ was employed for geometry optimisations and frequency computations. For all B3LYP⁶⁻⁹ and MP2¹⁰ computations we used the Gaussian16 program package. Intrinsic reaction paths were mapped using the Hessian based predictor-corrector integrator^{11, 12} and projected frequencies were computed along the path. WKB tunnelling computations were carried out with Wolfram Mathematica 10.3,¹³ CVT/SCT and CVT/ZCT computations with POLYRATE 2017^{14, 15} using Gaussrate 17-B as interface between Gaussian16 and POLYRATE. Instanton¹⁶ computations were performed with DL-FIND included in ChemShell.^{17, 18}

Synthesis.



Scheme S1: Synthesis of pyrolysis precursor ethyl 2-cyano-2-oxoacetate **10**.

1,2-Diethyl-1,2-dicyanofumarate (24):

Compound **24** was synthesized according to procedure by Ireland *et al.*¹⁹: 10.6 g (10 mL, 9.37 mmol) ethyl cyanoacetate, 19.7 g (12.0 mL, 165.0 mmol) SOCl_2 , 10 mL THF. Product **24** was obtained as colourless crystals:

Yield: 4.40 g (19.8 mmol, 42%).

$^1\text{H NMR}$ (400 MHz, CDCl_3): 4.48 (q, $J = 7.2$ Hz, 4H), 1.43 (t, $J = 7.1$ Hz, 5H) ppm.

$^{13}\text{C NMR}$ (101 MHz, CDCl_3): 157.7, 126.1, 111.4, 65.3, 13.9 ppm.

Spectroscopic data in accordance to the literature.²⁰

1,2-Diethoxycarbonyl-1,2-dicyanoethylene oxide (25):

Compound **25** was synthesized according to procedure by Linn *et al.*²¹: 3.03 g (13.6 mmol) **24**, 2.72 ml (26.6 mmol) 30% hydrogen peroxide, 3 drops pyridine, 15 ml MeCN.

Product **25** was obtained as colourless solid:

Yield: 2.26 g (9.49 mmol, 70%).

$^1\text{H NMR}$ (400 MHz, CDCl_3): 4.51 (qd, $J = 7.2$ Hz, 4.4 Hz, 42H), 4.40 (q, $J = 7.2$ Hz, 4H), 1.44 (t, $J = 7.2$ Hz, 6H), 1.38 (t, $J = 7.1$ Hz, 6H) ppm.

$^{13}\text{C NMR}$ (101 MHz, CDCl_3): 158.1, 157.6, 110.3, 109.5, 66.2, 65.7, 54.1, 53.2, 14.0, 13.9 ppm.

Ethyl 2-cyano-2-oxoacetate (10):

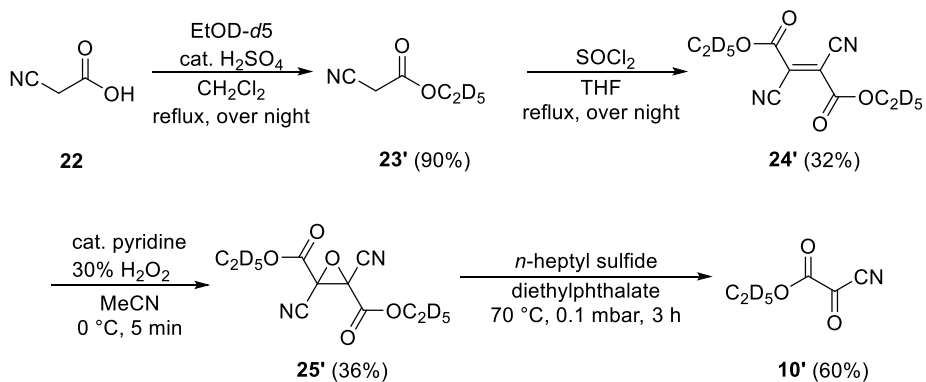
Compound **10** was synthesized according to procedure by Achmatowicz *et al.*²²: 0.450 g (1.89 mmol) **25**, 0.436 g (0.379 mL, 1.89 mmol) diheptyl sulfide, 1 mL diethylphthalate.

Product was obtained as yellow-greenish liquid.

Yield: $9.80 \cdot 10^{-3}$ g (0.771 mmol, 41%).

$^1\text{H NMR}$ (400 MHz, CD_2Cl_2): 4.48 (q, $J = 7.1$ Hz, 2H), 1.42 (t, $J = 7.2$ Hz, 2H) ppm.

$^{13}\text{C NMR}$ (101 MHz, CD_2Cl_2): 160.6, 156.5, 112.6, 66.0, 14.2 ppm.



Scheme S2: Synthesis of all deuterated pyrolysis precursor ethyl 2-cyano-2-oxoacetate **10'**.

2-Cyanoacetic acid ethyl-1,1,2,2,2-d5-ester (**23'**):

In a round-bottom flask equipped with an inverse Dean-Stark-Trap a mixture of 4.38 g (50.0 mmol) cyanoacetic acid **22**, 11.8 g (15.0 mL, 257 mmol) EtOD-d₅ and 0.045 g (0.082 mL, 0.454 mmol) conc. H₂SO₄ in 190 ml of CH₂Cl₂ was refluxed over night. The mixture was washed with 100 ml of 8 wt.% sodium bicarbonate-solution, the aqueous phase was extracted three times, each with 100 ml CH₂Cl₂ and dried over Na₂SO₄. The product **23'** was obtained as a colourless oil.

Yield: 5.30 g (44.9 mmol, 90%).

¹H NMR (400 MHz, CDCl₃): 3.45 (s, 2H) ppm.

¹³C NMR (101 MHz, CDCl₃): 163.0, 113.2, 62.4 (p, *J* = 22.5 Hz), 24.9, 13.1 (p, *J* = 19.2 Hz) ppm.

IR (ATR): ν = 2264.5, 1737.4, 1398.5, 1347.7, 1286.6, 1224.5, 1185.5, 1092.5, 1059.2, 1049.7, 1022.1, 985.9, 936.3 896.4, 709.6, 578.8 cm⁻¹.

HRMS (ESI): *m/z* = 141.0635 [M+Na]⁺ (calcd *m/z* = 141.0633).

All-deutero-1,2-Diethyl-1,2-dicyanofumarate (**24'**):

To a solution of 9.85 g (6 mL, 8.25 mmol) SOCl₂ in 5 mL THF 5.00 g (4.72 mL, 4.23 mmol) **23'** were added over a period of 5 minutes. The mixture was refluxed for 3 hours, cooled to r.t. and crystallized over night at 3 °C. The crude product was filtered, washed with cold EtOH and recrystallized from a small amount of EtOH. The product **24'** was obtained as fine colourless needles.

Yield: 1.53 g (6.80 mmol, 32%).

¹H NMR (400 MHz, CDCl₃): –.

¹³C NMR (101 MHz, CDCl₃): 157.8, 126.1, 111.4 64.6 (p, *J* = 22.8 Hz), 12.9 (p, *J* = 19.2 Hz) ppm.

IR (ATR): ν = 2228.7, 1725.7 1557.0m 1283.7, 1186.2, 1085.3, 1057.5, 1042.5, 957.6, 918.2, 860.5, 736.5, 738.6, 592.8, 507.0 cm⁻¹.

HRMS (ESI): *m/z* = 255.1158 [M+Na]⁺ (calcd *m/z* = 255.1160).

All-deutero-1,2-Dioethoxycarbonyl-1,2-dicyanoethylene Oxide (**25'**):

To a solution of 0.750 g (3.23 mmol) **24'** in THF 0.673 ml (6.59 mmol) 30% hydrogen peroxide followed by a droplet of pyridine were added. The mixture was stirred for 5 minutes and immediately put onto a vigorously stirred water-ice mixture. The separated oil crystallized upon repeated stirring and scratching. The solid residue was filtered, dissolved in boiling diethylether and the product was precipitated by addition of *n*-pentane. The product **25'** was obtained as a colourless solid.

Yield: 0.29 g (1.17 mmol, 36%).

¹H NMR (400 MHz, CDCl₃): –.

^{13}C NMR (101 MHz, CDCl_3): 158.1, 109.5, 65.4 (t, $J = 23.1$ Hz), 53.2, 13.0 (p, $J = 20.2$ Hz) ppm.
IR (ATR): $\nu = 2243.6, 1744.7, 1486.5, 1321.9, 1196.3, 1105.8, 1087.0, 1046.5, 993.7, 948.3, 927.9, 882.7, 770.2, 727.7, 641.6, 581.1, 478.3, 445.5 \text{ cm}^{-1}$.
HRMS (ESI): $m/z = 271.1107$ [M+Na] $^+$ (calcd $m/z = 271.1109$).

All-deutero-Ethyl 2-cyano-2-oxoacetate (10'**):**

In a 2-neck flask equipped with a Vigreux column and a dropping funnel 0.240 g (0.968 mmol) **25'** were dissolved in 0.5 mL diethylphthalate under Schlenk conditions. The pressure was reduced to 0.5 mbar while heating to 50°C. 0.230 g (0.200 mL, 0.998· mmol) diheptyl sulfide was added dropwise over 20 minutes. After completion the mixture was heated to 70 °C for 3 hours. The product was collected as a white solid in the receiver cooled with liquid nitrogen. After warming the receiver to r.t. under N_2 -atmosphere the product **10'** was obtained as a yellow-greenish liquid.

Yield: 0.038 g (0.288 mmol, 60%).

^1H NMR (600 MHz, CDCl_3): –.

^2H NMR (600 MHz, CDCl_3): 4.45 (d, $J = 6.4$ Hz, 2D), 1.40 (d, $J = 2.4$ Hz, 3D) ppm.

^{13}C NMR (101 MHz, CDCl_3 , not enough intensity to see C–D-coupling): 159.8, 155.8, 111.9, 63.8, 12.8 ppm.

IR (Ar-Matrix, 3 K): $\nu = 2233, 1784, 1755, 1735, 1341, 1298, 1283, 1210, 1206, 1100, 1087, 1074, 1059, 1052, 980, 968, 822, 497 \text{ cm}^{-1}$.

NMR spectra were recorded on Bruker AV400 and AV600 spectrometers at 298 K. Chemical shifts (δ) are given in ppm relative to tetramethylsilane (TMS, $\delta = 0.00$ ppm) as the internal standard or to the respective solvent residual peaks (CDCl_3 : $\delta = 7.26$ and 77.16 ppm; CD_2Cl_2 : $\delta = 5.33$ and 54.24 ppm). High resolution mass spectrometry was performed with a Bruker MicrOTOF (positive mode ESI-MS). ATR-IR spectra were recorded on a Bruker Alpha spectrometer (4000 – 400 cm^{-1}).

NMR Spectra

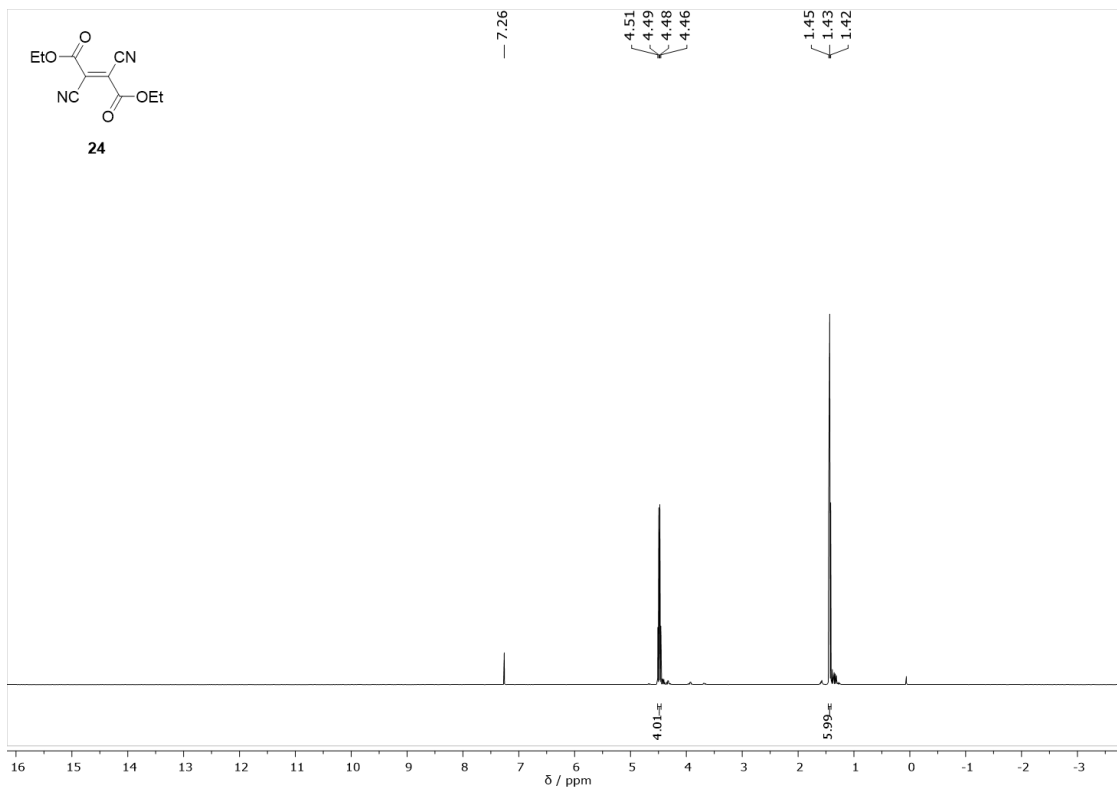


Figure S1: ¹H NMR (400 MHz, CDCl₃) of 1,2-diethyl-1,2-dicyanofumarate (**24**).

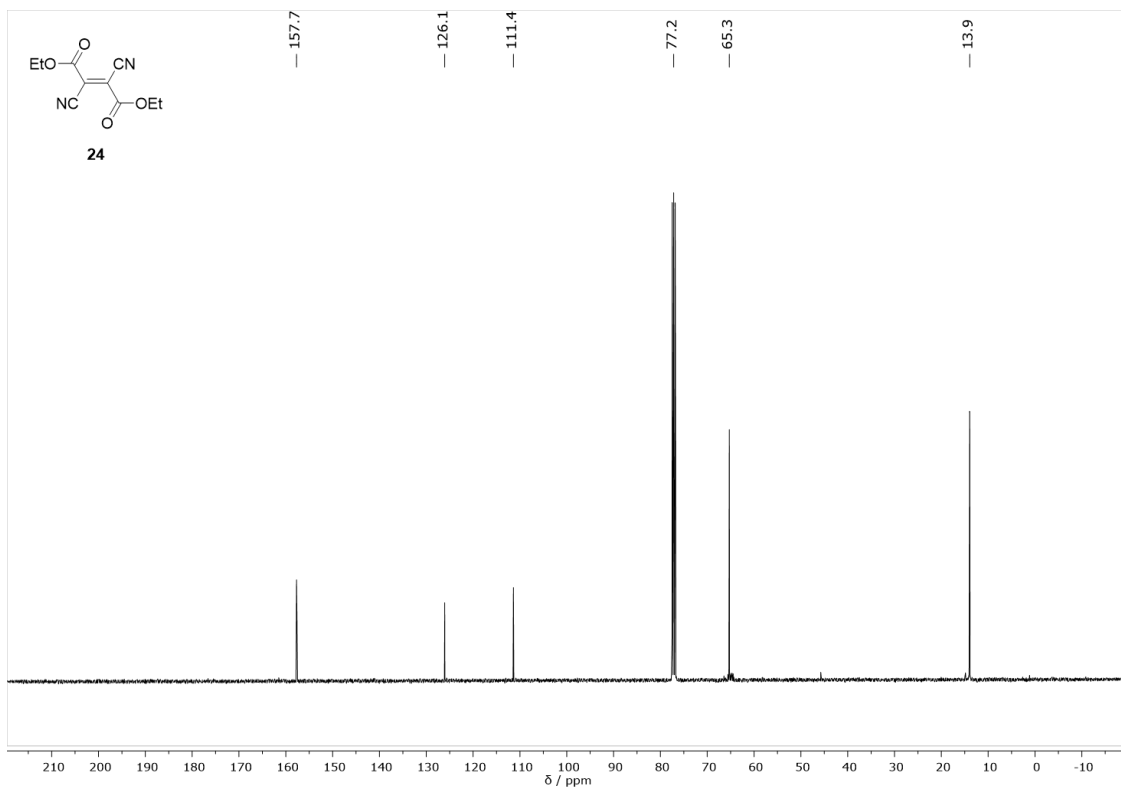


Figure S2: ¹³C NMR (101 MHz, CDCl₃) of 1,2-diethyl-1,2-dicyanofumarate (**24**).

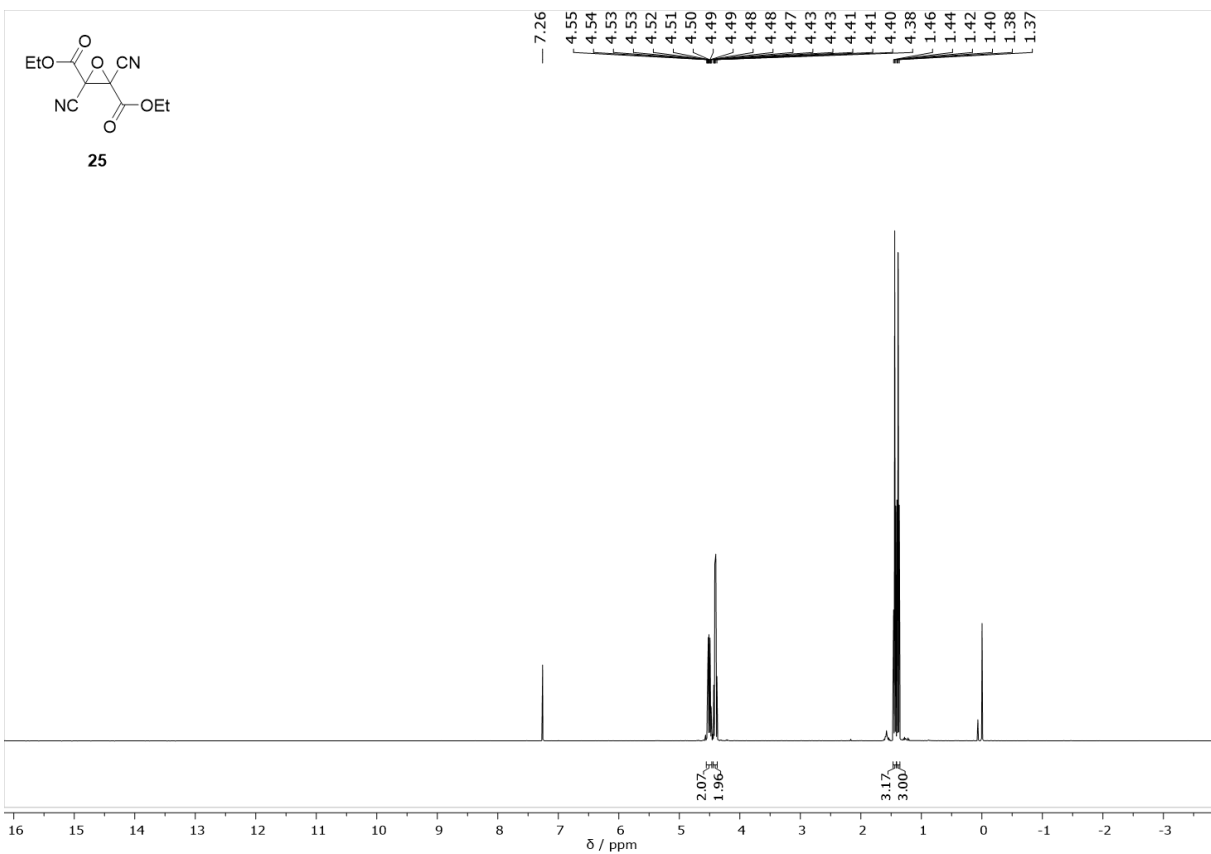


Figure S3: ^1H NMR (400 MHz, CDCl_3) of 1,2-diethoxycarbonyl-1,2-dicyanoethylene oxide (**25**).

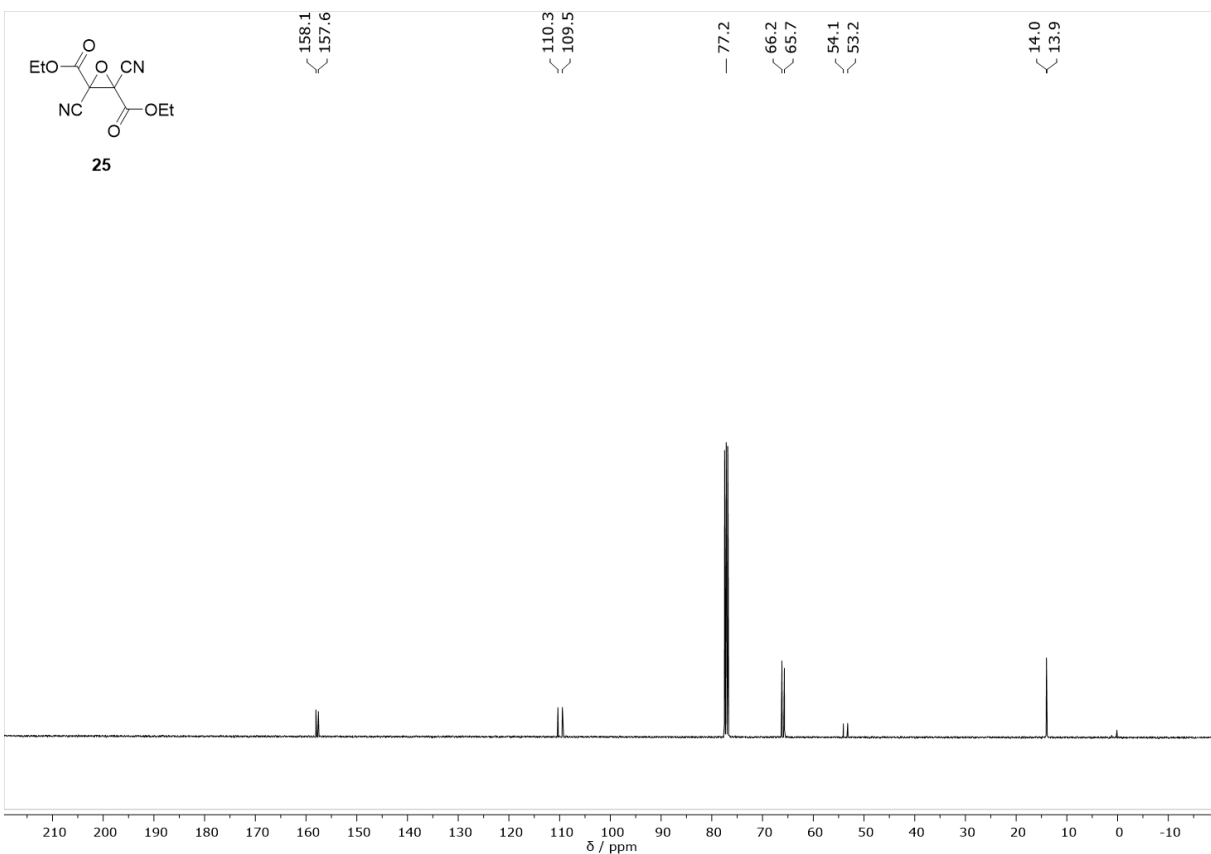


Figure S4: ^{13}C NMR (101 MHz, CDCl_3) of 1,2-diethoxycarbonyl-1,2-dicyanoethylene oxide (**25**).

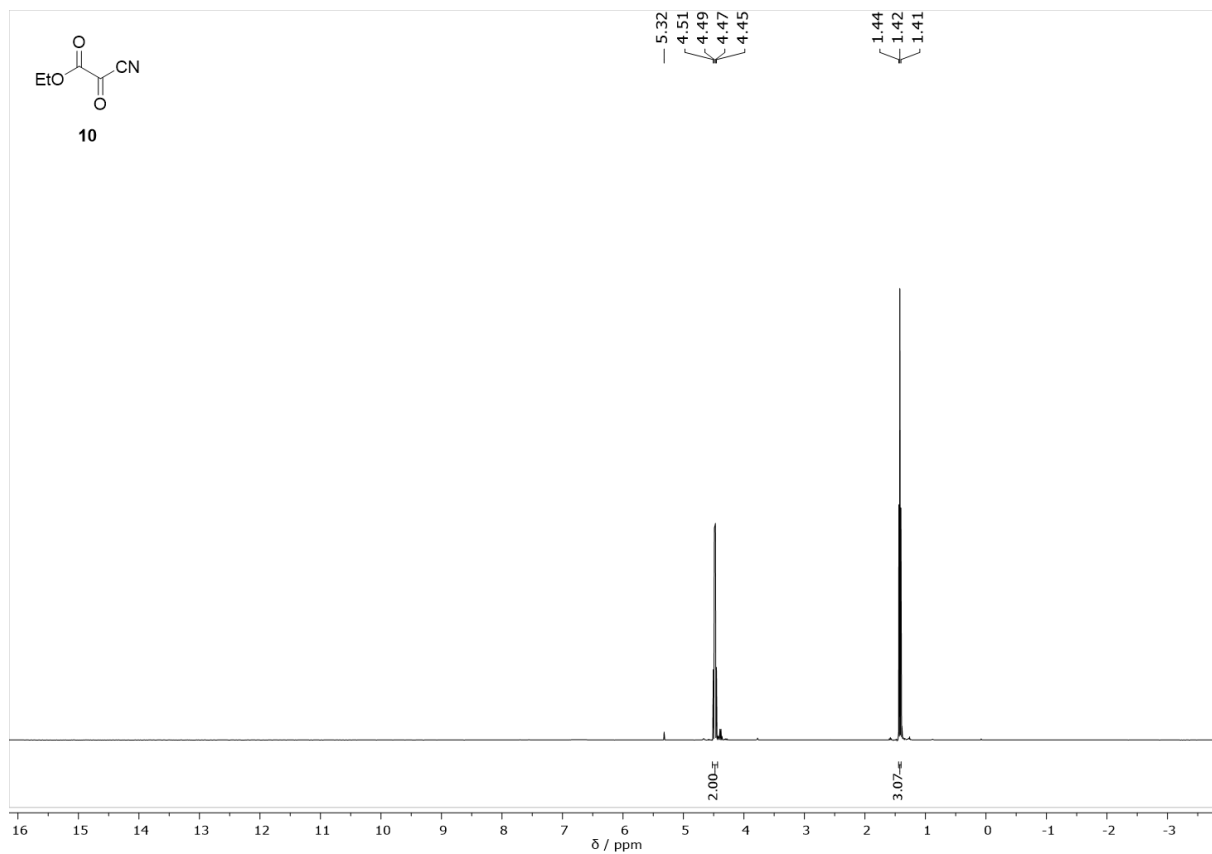


Figure S5: ¹H NMR (400 MHz, CD₂Cl₂) of ethyl 2-cyano-2-oxoacetate (**10**).

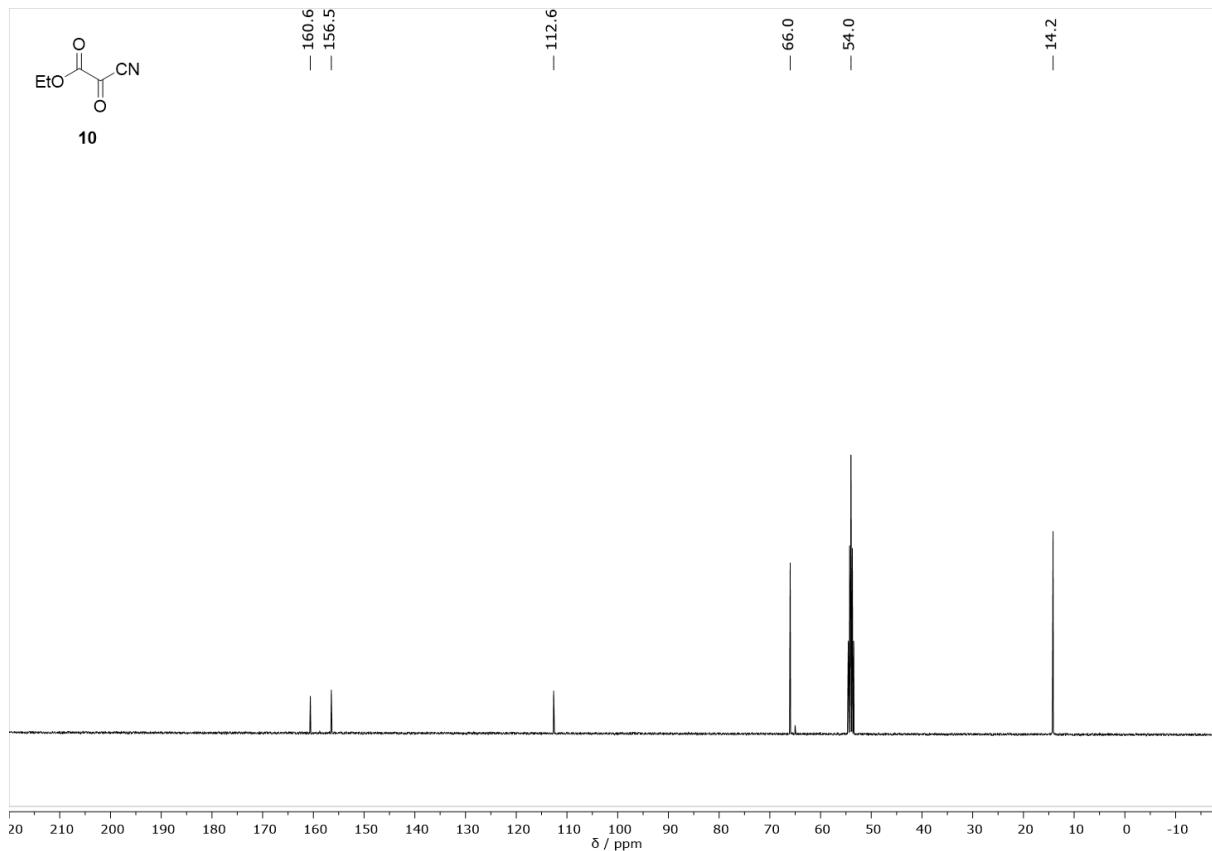


Figure S6: ¹³C NMR (101 MHz, CD₂Cl₂) of ethyl 2-cyano-2-oxoacetate (**10**).

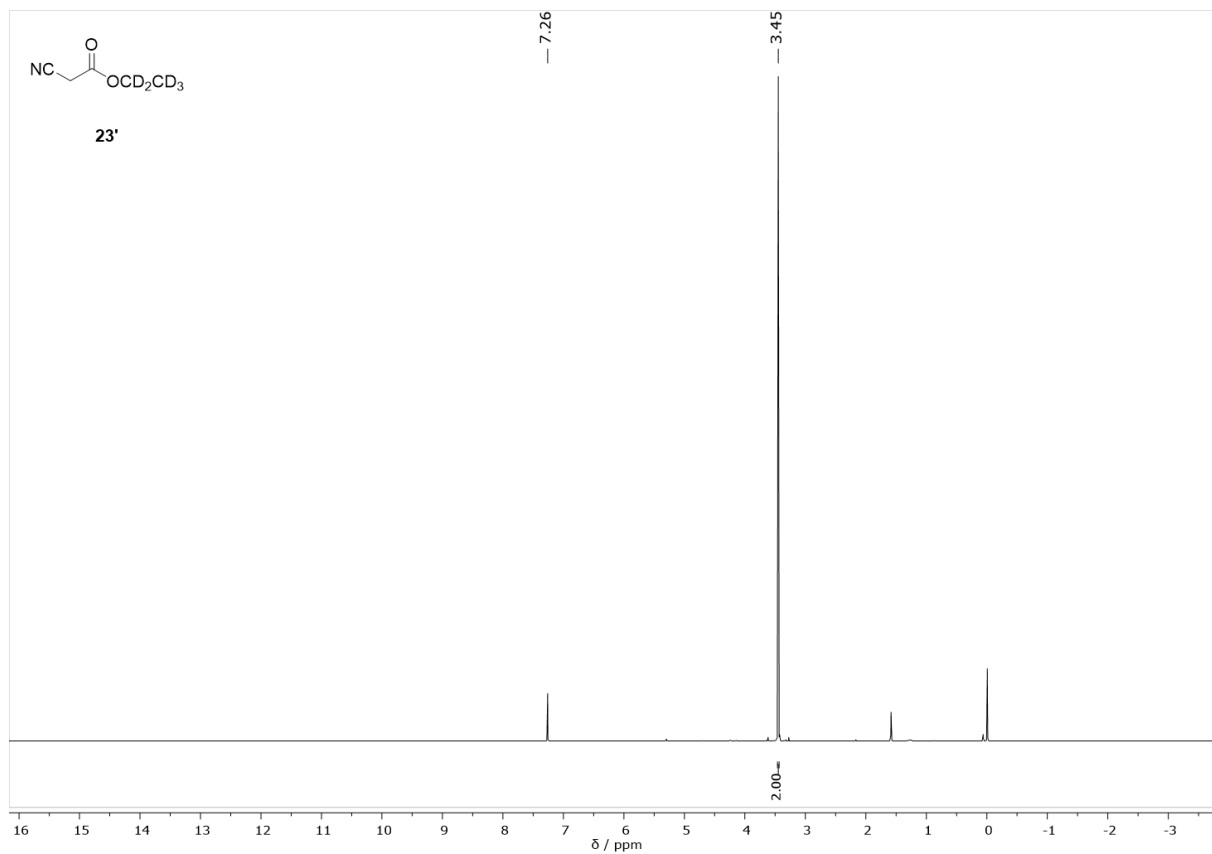


Figure S7: ^1H NMR (400 MHz, CDCl_3) of 2-cyanoacetic acid ethyl-1,1,2,2-d₅-ester (**23'**).

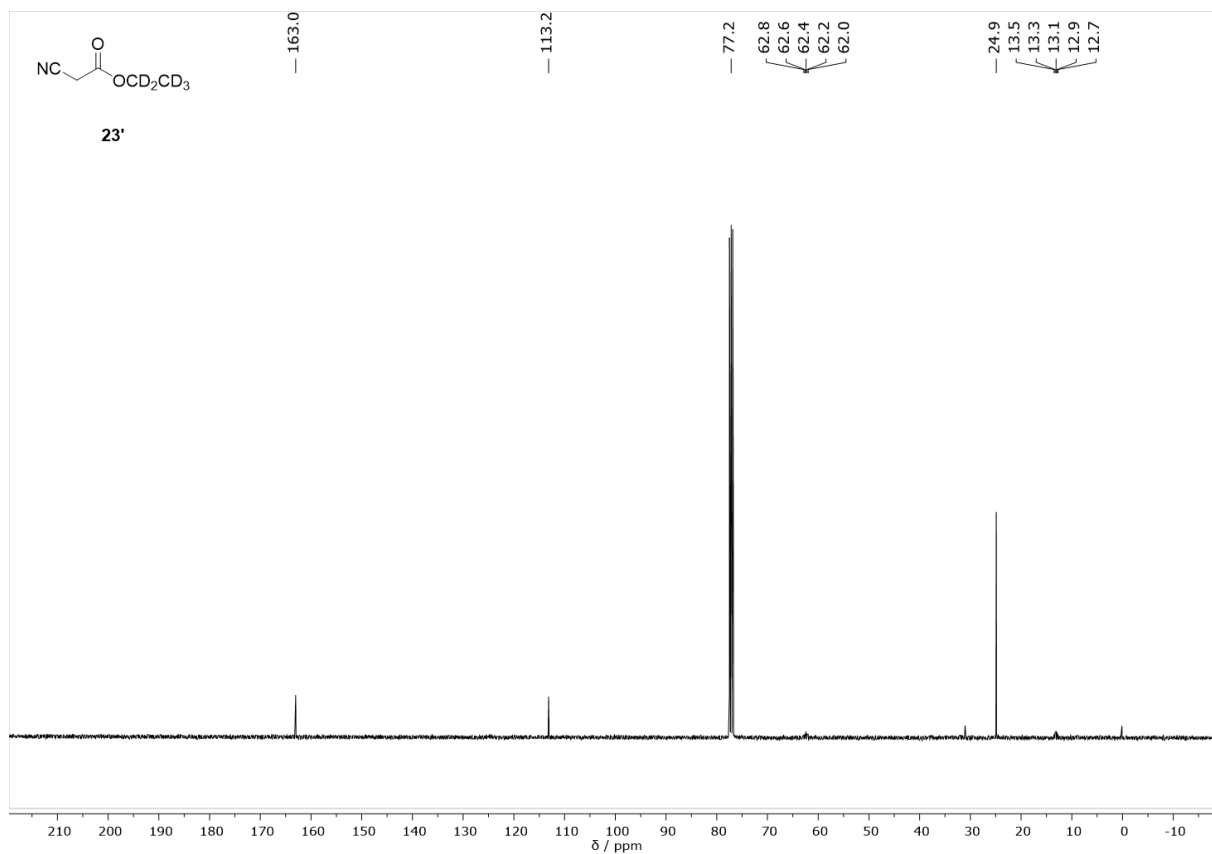


Figure S8: ^{13}C NMR (101 MHz, CDCl_3) of 2-cyanoacetic acid ethyl-1,1,2,2-d₅-ester (**23'**).

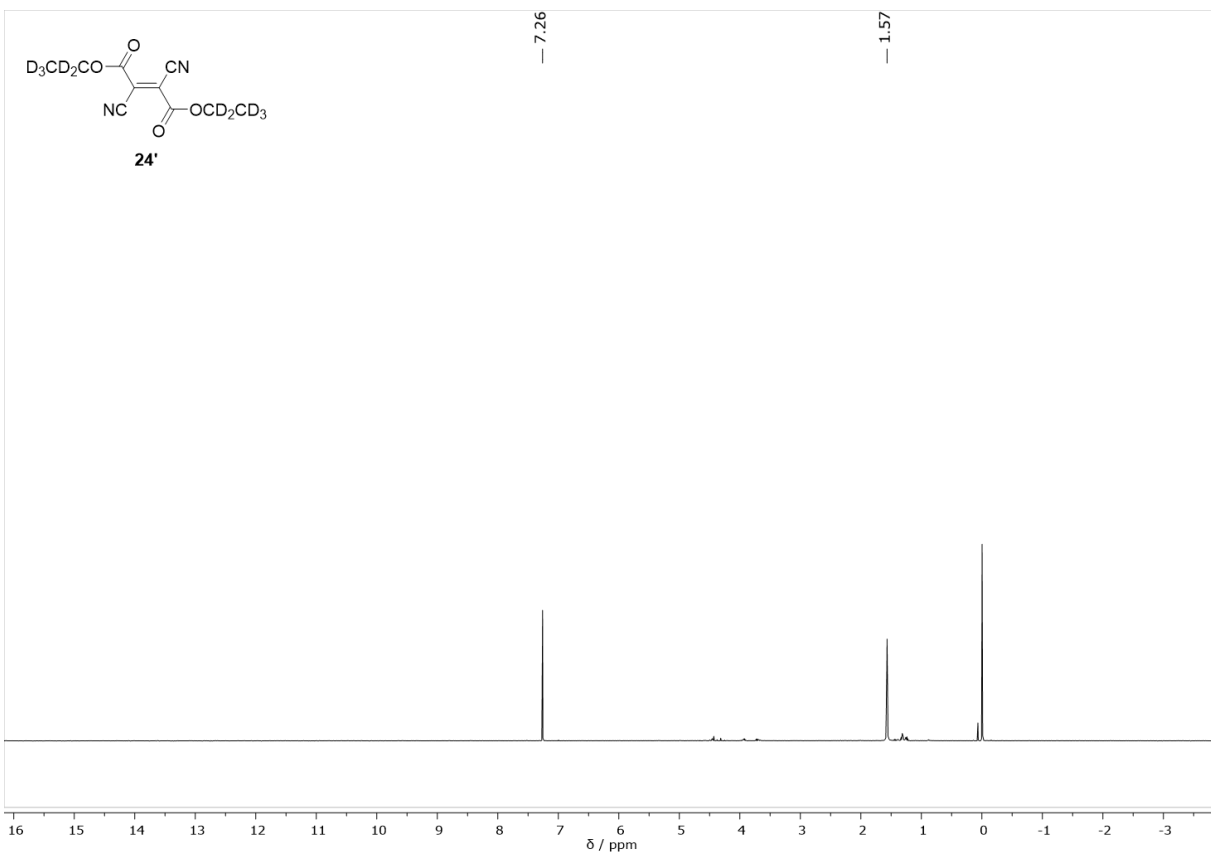


Figure S9: ^1H NMR (400 MHz, CDCl_3) of *all*-deutero-1,2-diethyl-1,2-dicyanofumarate (**24'**).

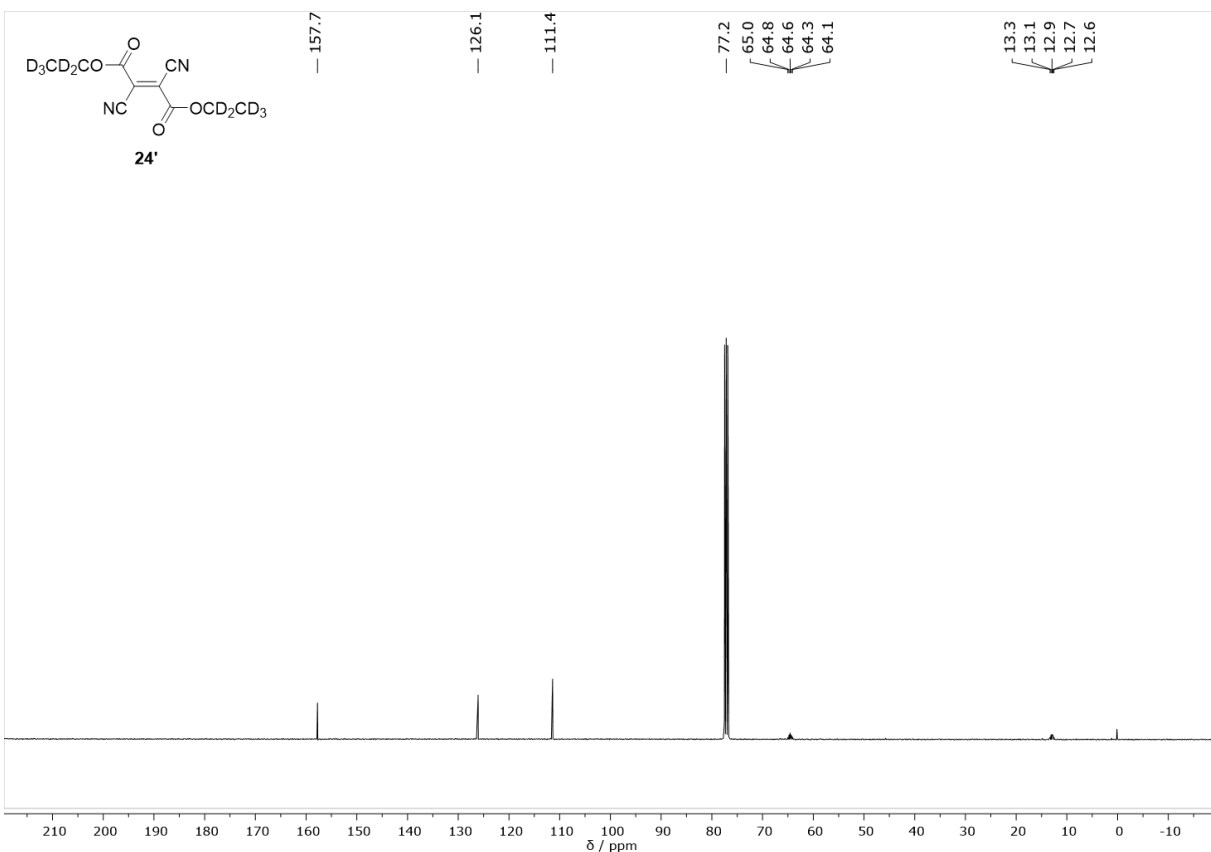


Figure S10: ^{13}C NMR (101 MHz, CDCl_3) of *all*-deutero-1,2-diethyl-1,2-dicyanofumarate (**24'**).

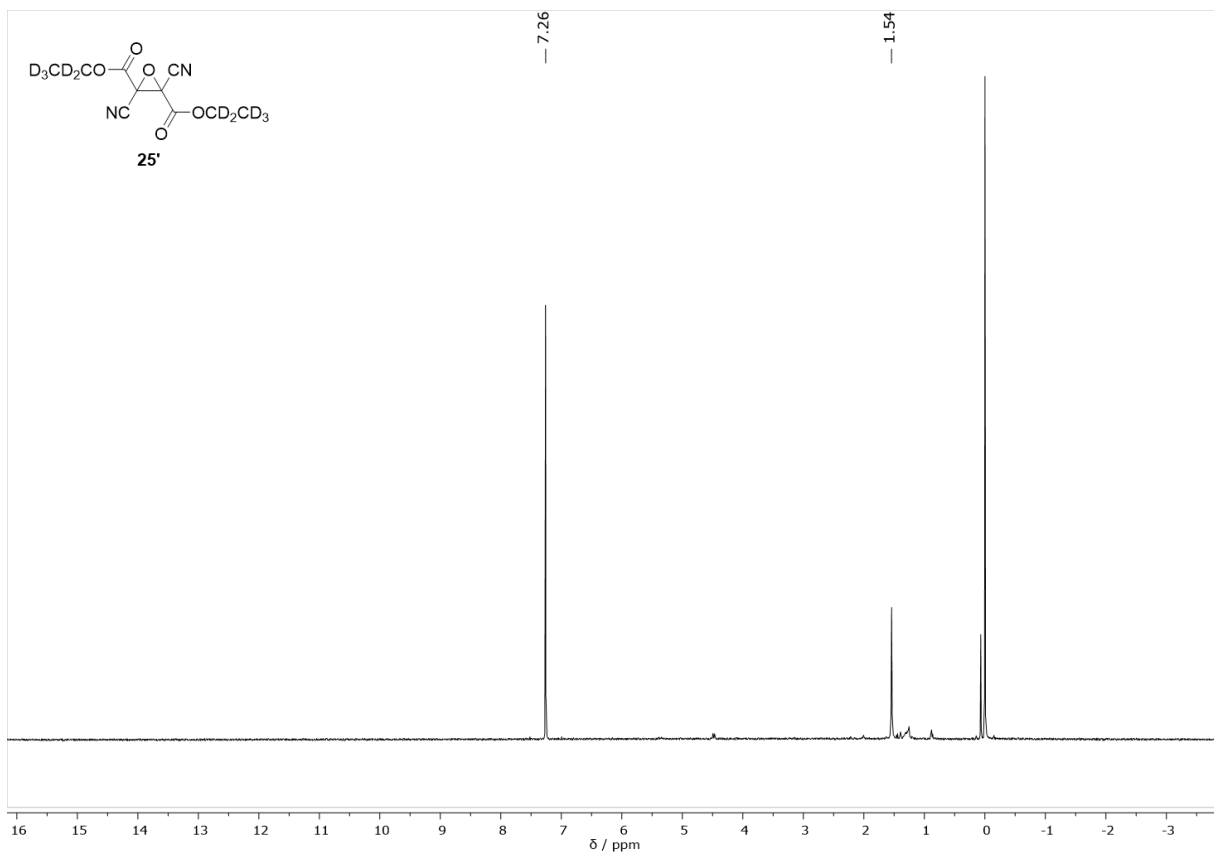


Figure S11: ^1H NMR (400 MHz, CDCl_3) of *all*-deutero-1,2-diethoxycarbonyl-1,2-dicyanoethylene oxide (**25'**).

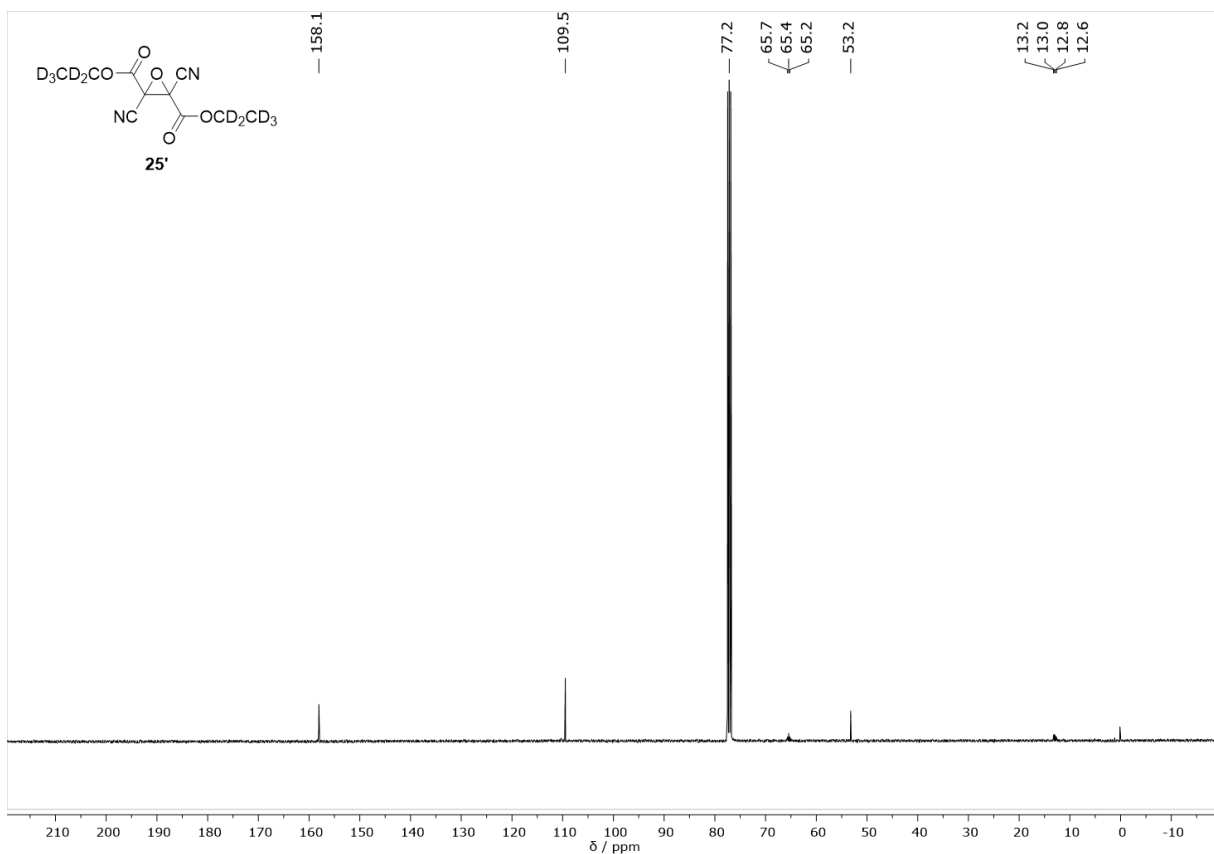


Figure S12: ^{13}C NMR (101 MHz, CDCl_3) of *all*-deutero-1,2-diethoxycarbonyl-1,2-dicyanoethylene oxide (**25'**).

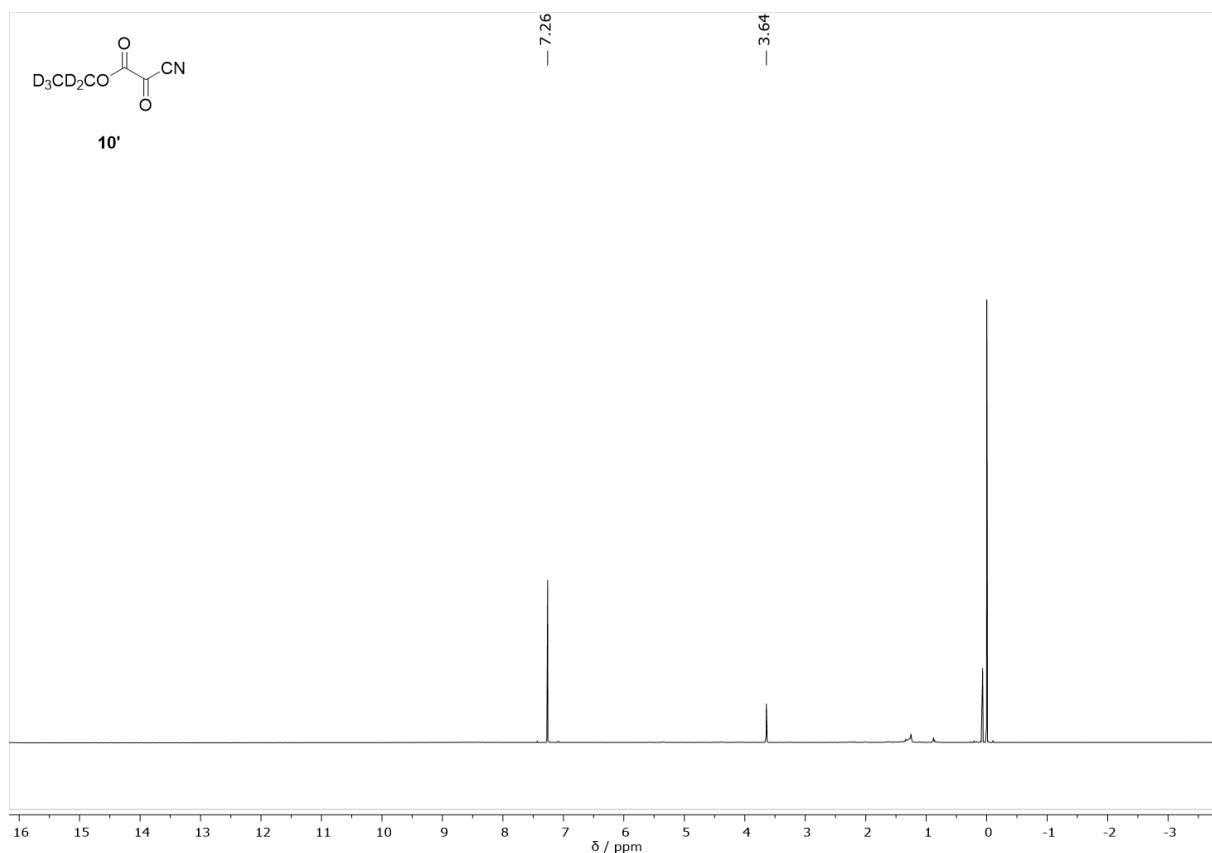


Figure S13: ^1H NMR (600 MHz, CDCl_3) of *all*-deutero-ethyl 2-cyano-2-oxoacetate (**10'**).

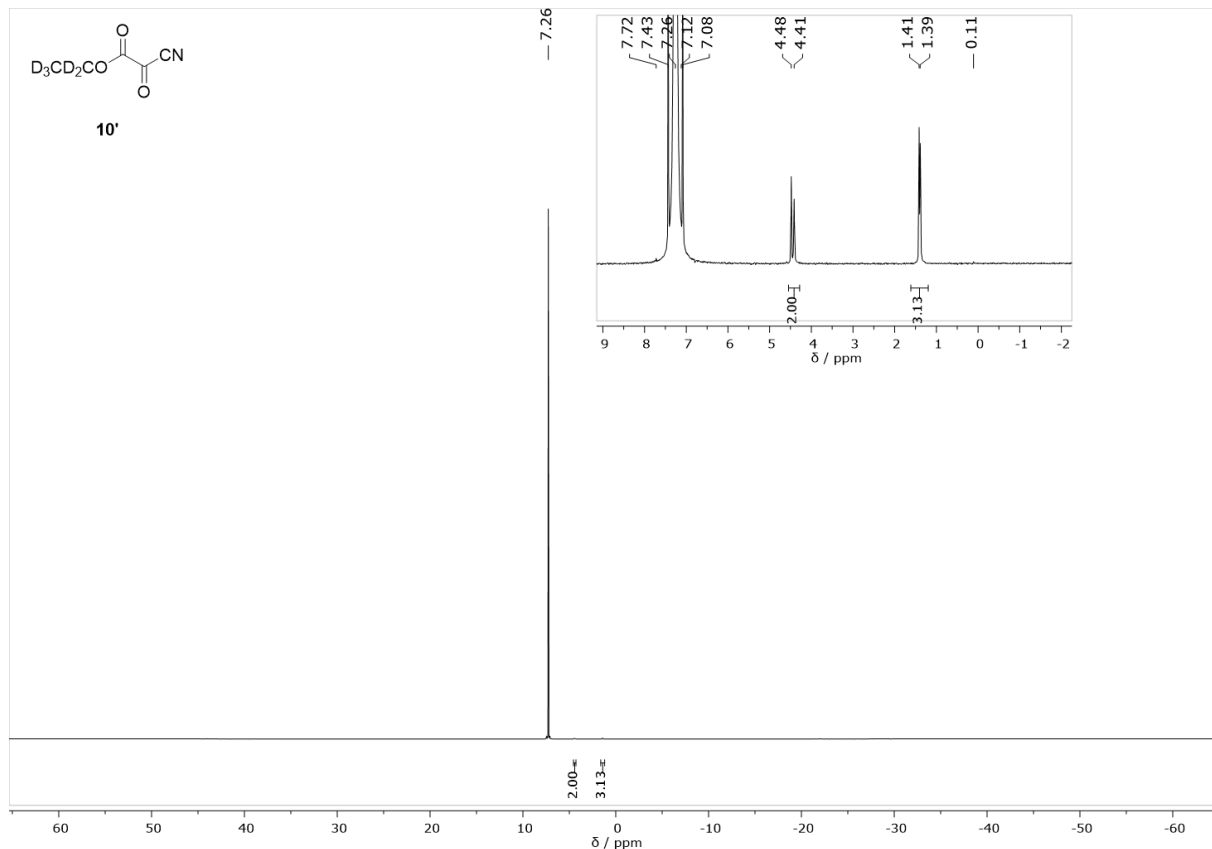


Figure S14: ^2H NMR (600 MHz, CDCl_3) of *all*-deutero-ethyl 2-cyano-2-oxoacetate (**10'**).

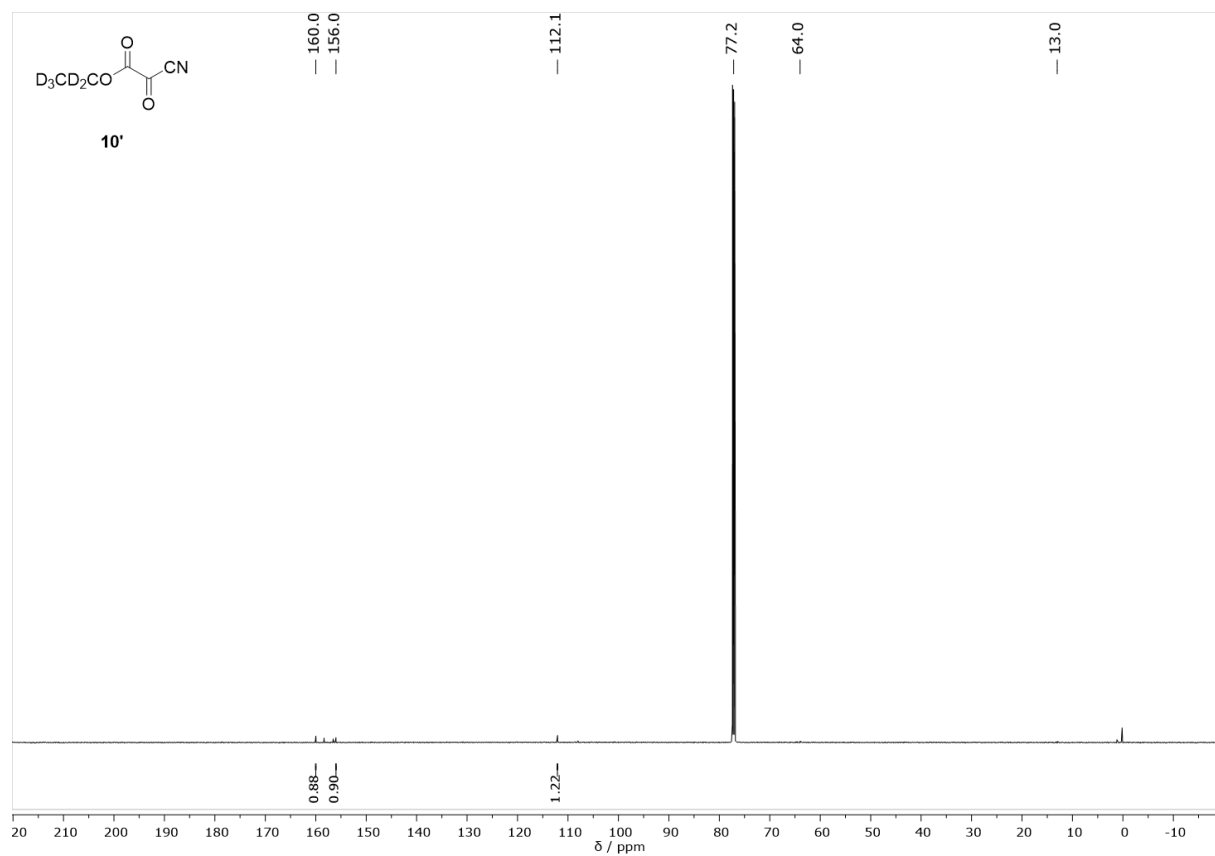


Figure S15: ^{13}C NMR (101 MHz, CDCl_3) of *all*-deutero-ethyl 2-cyano-2-oxoacetate ($\mathbf{10}'$).

Infrared Spectra

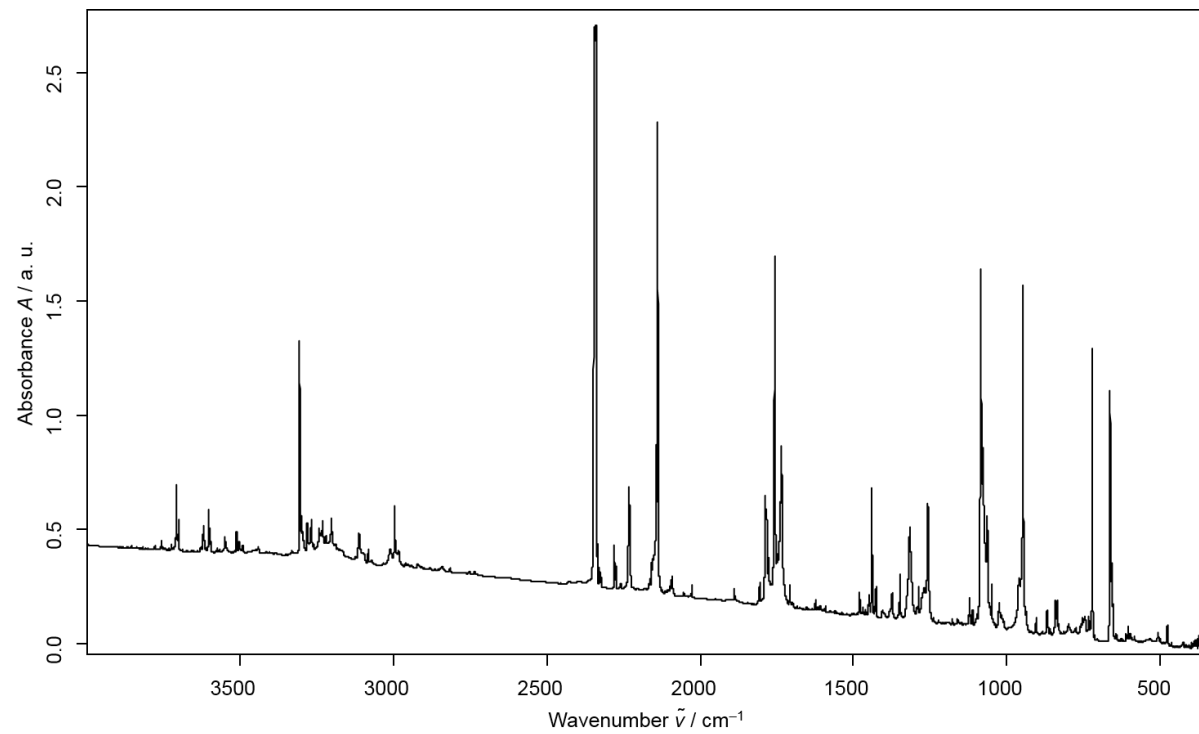


Figure S16: IR-spectrum recorded after 4 h pyrolysis of **10** at 900 °C and subsequent matrix isolation of the pyrolysis products in solid Ar.

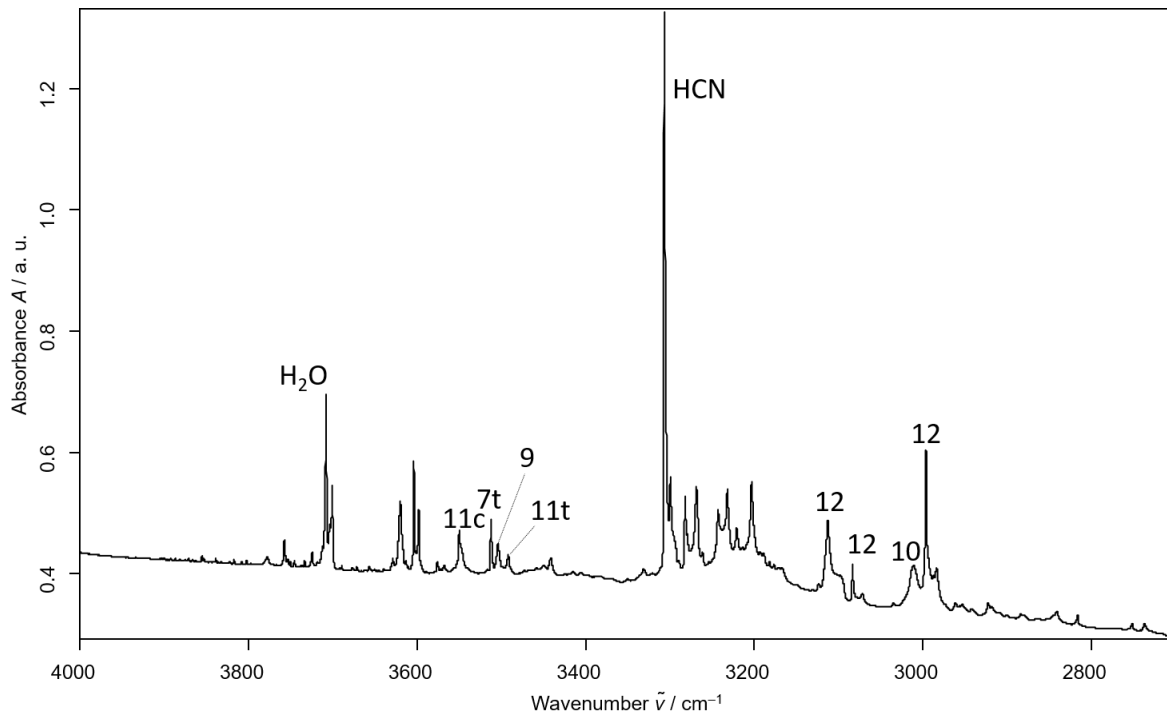


Figure S17: IR-spectrum in the range of 4000 – 2700 cm⁻¹ recorded after 4 h pyrolysis of **10** at 900 °C and subsequent matrix isolation of the pyrolysis products in solid Ar.

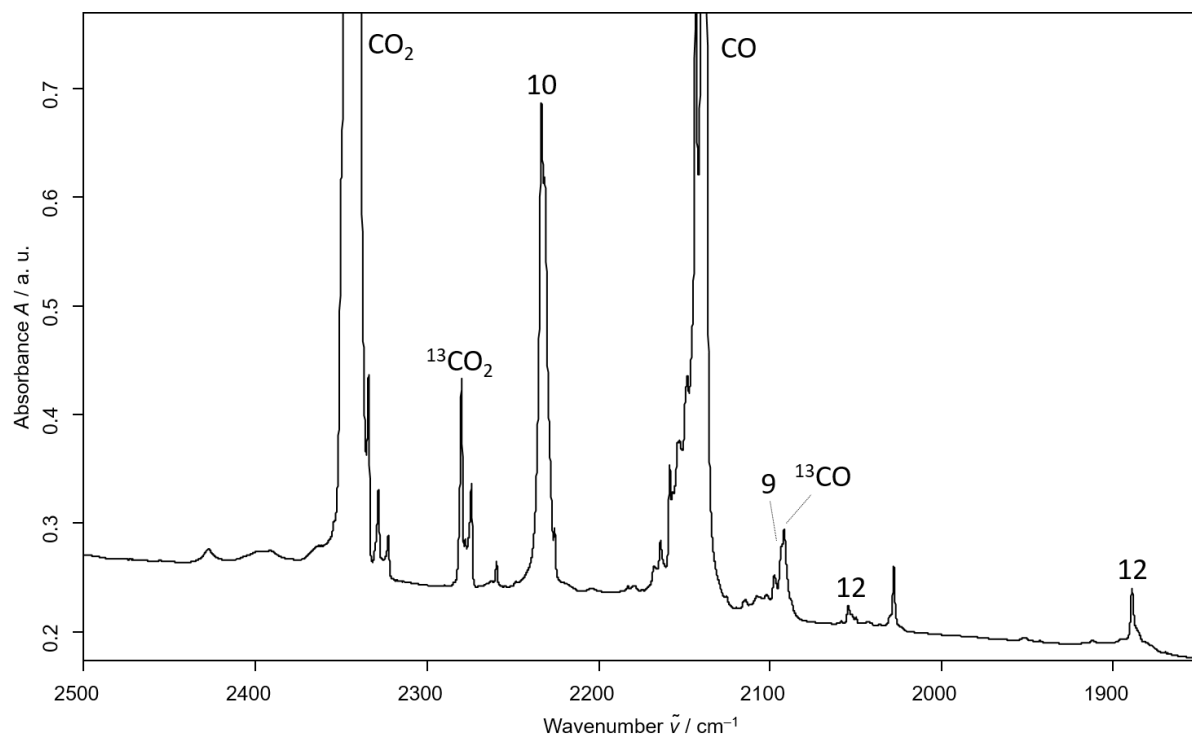


Figure S18: IR-spectrum in the range of $2500 - 1850 \text{ cm}^{-1}$ recorded after 4 h pyrolysis of **10** at $900 \text{ }^\circ\text{C}$ and subsequent matrix isolation of the pyrolysis products in solid Ar.

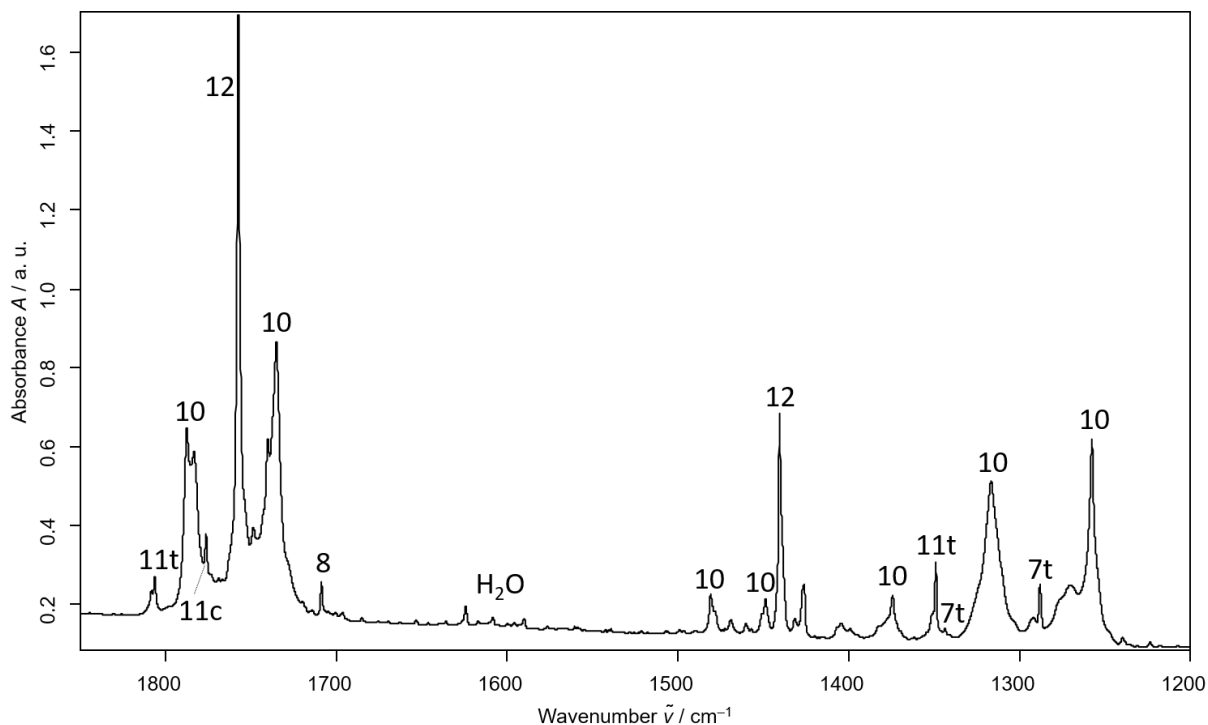


Figure S19: IR-spectrum in the range of $1850 - 1200 \text{ cm}^{-1}$ recorded after 4 h pyrolysis of **10** at $900 \text{ }^\circ\text{C}$ and subsequent matrix isolation of the pyrolysis products in solid Ar.

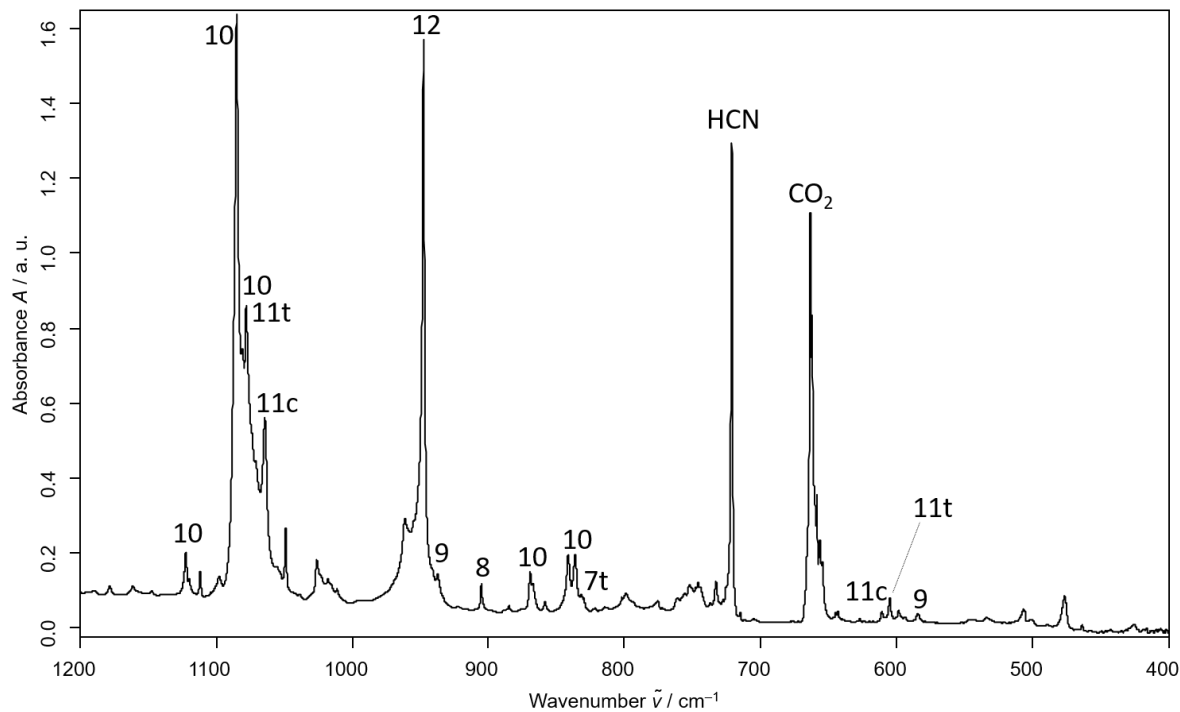


Figure S20: IR-spectrum in the range of $1200 - 400 \text{ cm}^{-1}$ recorded after 4 h pyrolysis of **10** at $900 \text{ }^\circ\text{C}$ and subsequent matrix isolation of the pyrolysis products in solid Ar.

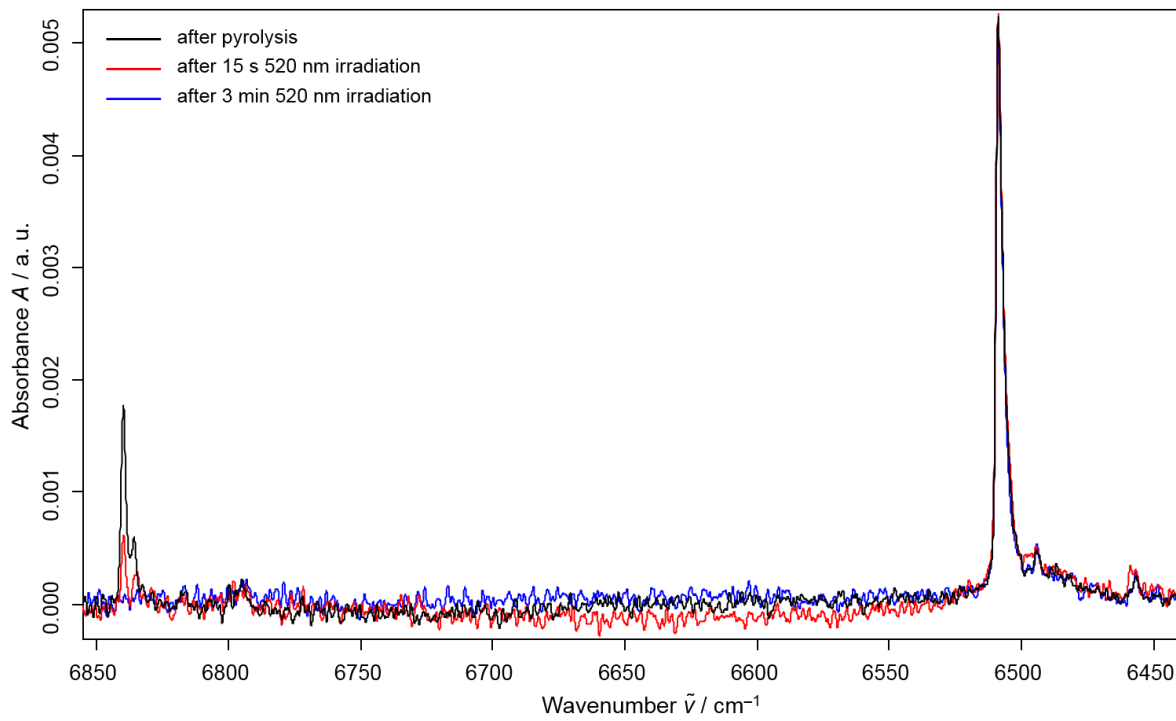


Figure S21: NIR-spectrum recorded after 4 h pyrolysis of **10** at $900 \text{ }^\circ\text{C}$ and subsequent matrix isolation of the pyrolysis products in solid Ar. By irradiation of the matrix with green light (520 nm) for a few minutes the O–H stretching overtone of **7t** disappears at around 6848 cm^{-1} .

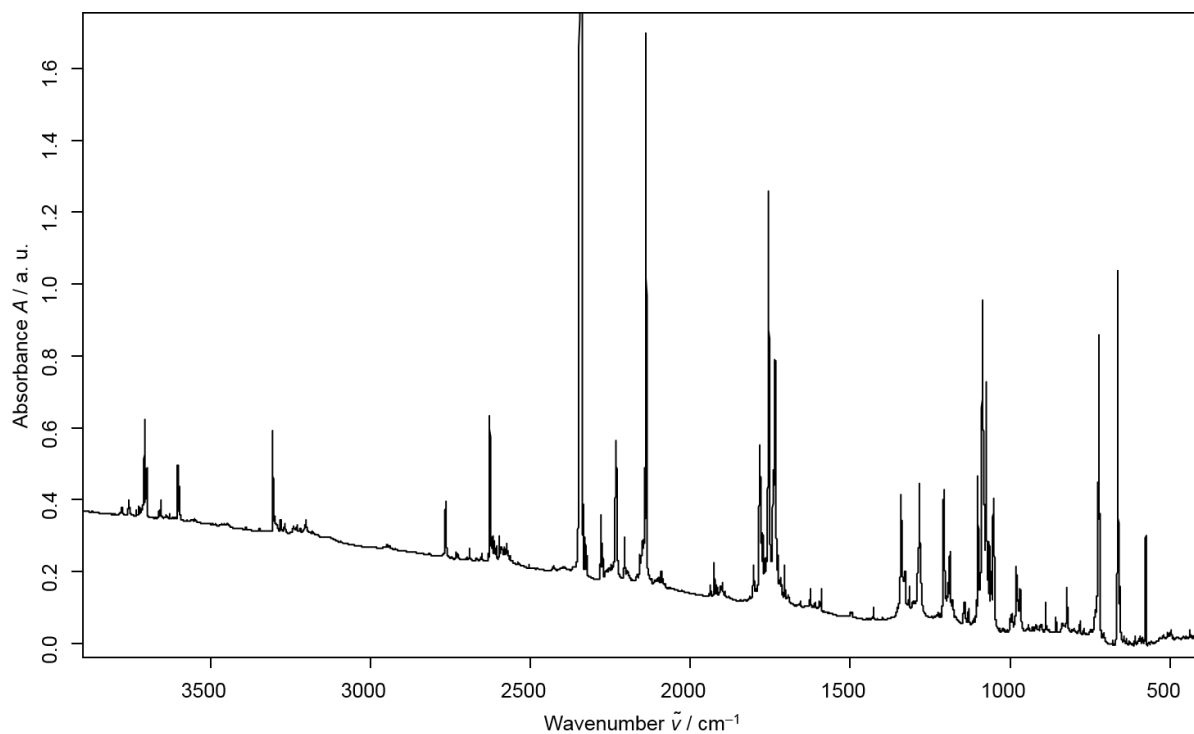


Figure S22: IR-spectrum recorded after 4 h pyrolysis of fully deuterated **10'** at 900 °C and subsequent matrix isolation of the pyrolysis products in solid Ar.

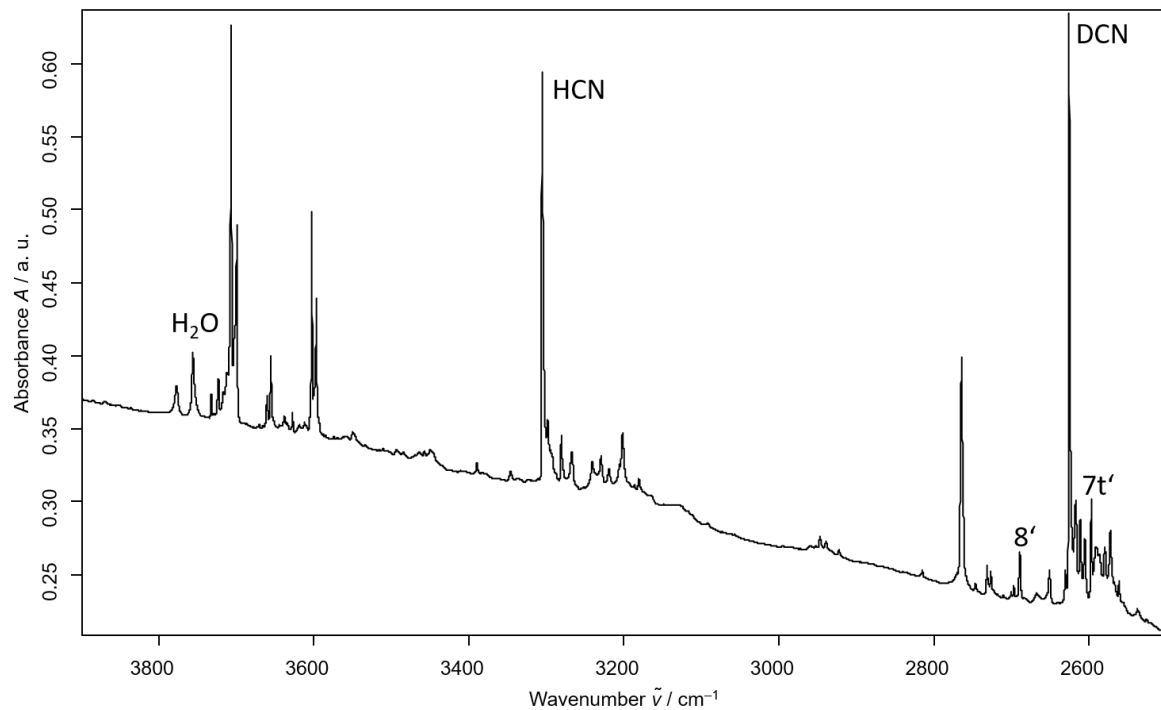


Figure S23: IR-spectrum in the range of 4000 – 2500 cm⁻¹ recorded after 4 h pyrolysis of fully deuterated **10'** at 900 °C and subsequent matrix isolation of the pyrolysis products in solid Ar.

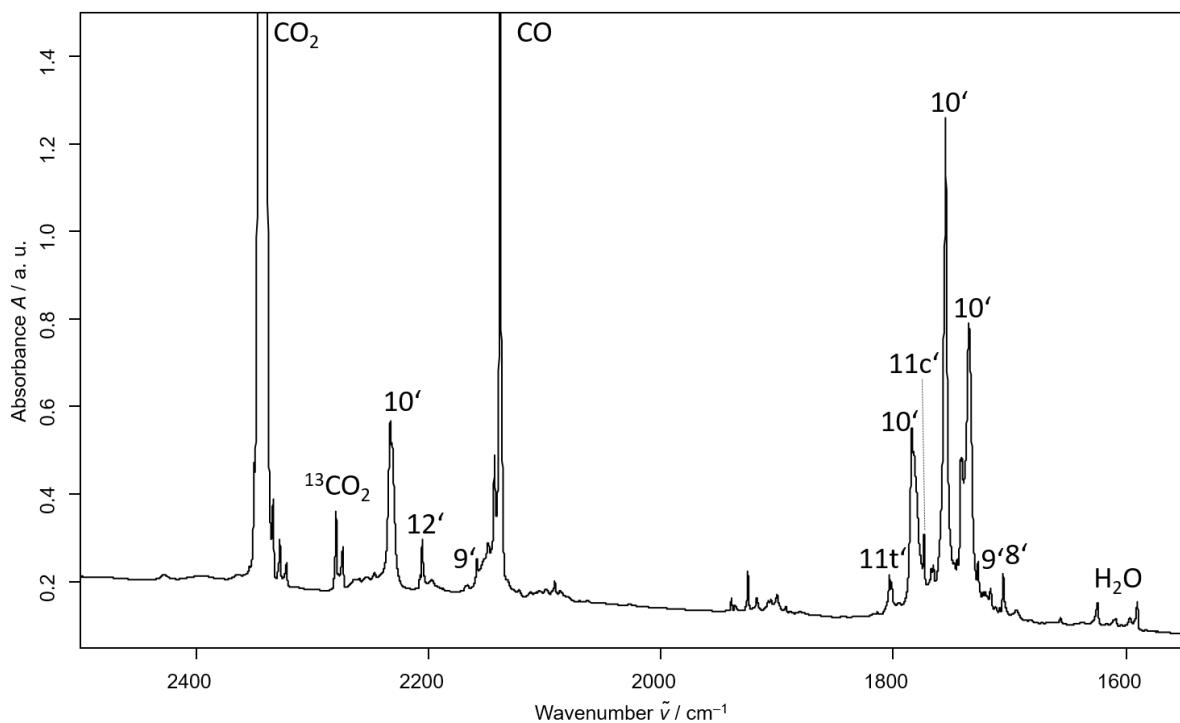


Figure S24: IR-spectrum in the range of $2500 - 1550 \text{ cm}^{-1}$ recorded after 4 h pyrolysis of fully deuterated **10'** at $900 \text{ }^\circ\text{C}$ and subsequent matrix isolation of the pyrolysis products in solid Ar.

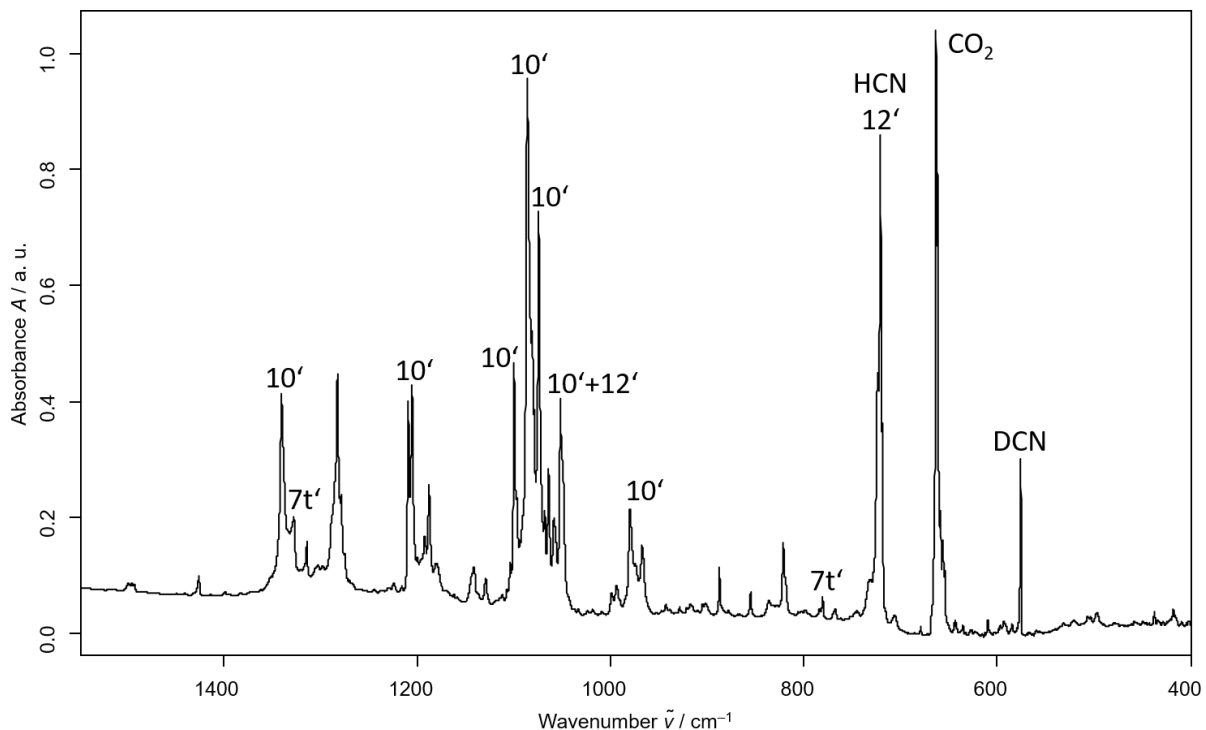


Figure S25: IR-spectrum in the range of $1500 - 400 \text{ cm}^{-1}$ recorded after 4 h pyrolysis of fully deuterated **10'** at $900 \text{ }^\circ\text{C}$ and subsequent matrix isolation of the pyrolysis products in solid Ar.

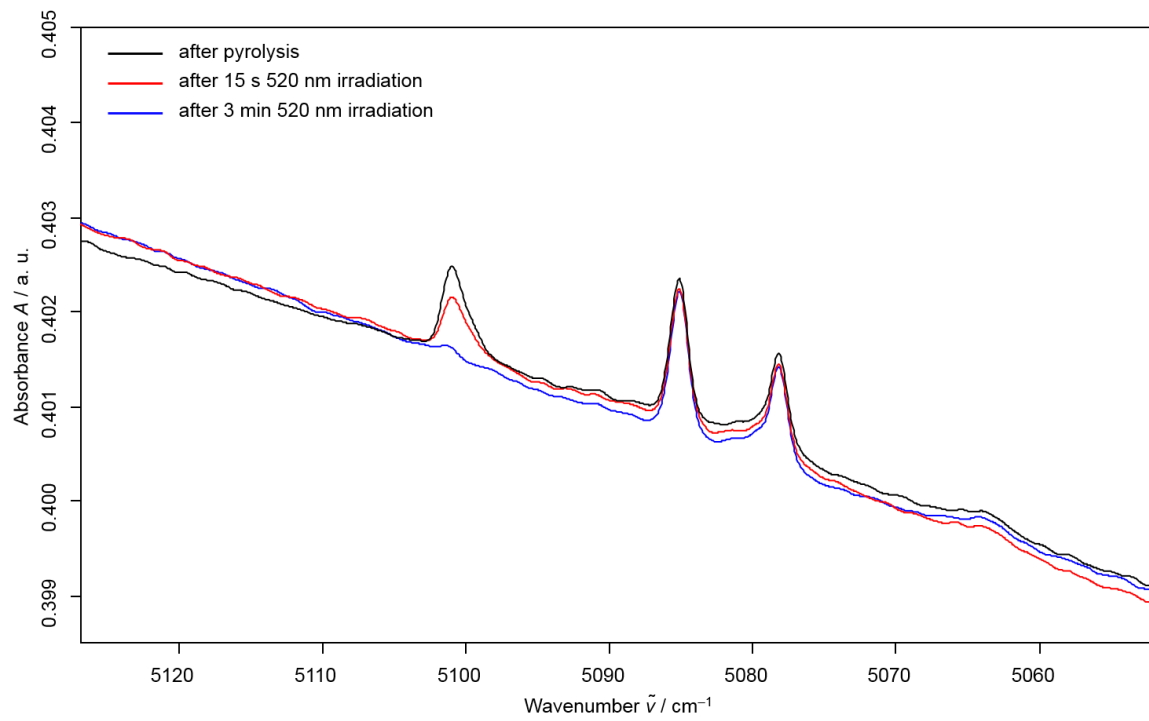


Figure S26: NIR-spectrum recorded after 4 h pyrolysis of fully deuterated **10'** at 900 °C and subsequent matrix isolation of the pyrolysis products in solid Ar. By irradiation of the matrix with green light (520 nm) for a few minutes the O–D stretching overtone of deuterated **7t'** disappears at around 5103 cm^{−1}.

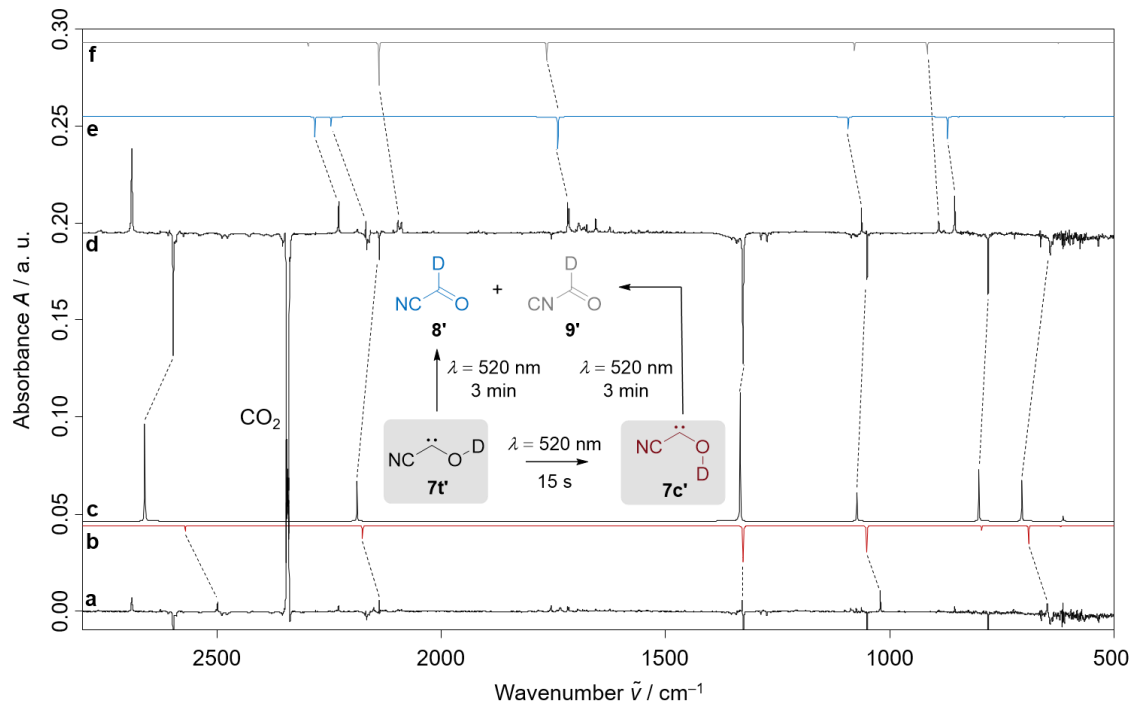


Figure S27: a: Experimental difference spectrum between the spectra recorded after 15 s irradiation of the matrix with a wavelength of 520 nm and the spectra immediately recorded after 4 h pyrolysis of fully deuterated ethyl 2-cyano-2-oxoacetate (**10'**) at 900 °C; b and c: Computed anharmonic AE-CCSD(T)/cc-pCVQZ vibrational spectra (unscaled) of deuterated *cis*-cyanohydroxycarbene-*O*-*D* (**7c'**, red, b) and *trans*-cyanohydroxycarbene-*O*-*D* (**7t'**, black, c); d: Experimental difference spectrum between the spectra recorded after 3 min irradiation of the matrix with a wavelength of 520 nm and the spectra immediately recorded after 4 h pyrolysis of fully deuterated ethyl 2-cyano-2-oxoacetate (**10'**) at 900 °C; e and f: Computed harmonic AE-CCSD(T)/cc-pCVQZ vibrational spectra (unscaled) of deuterated isocyanoformaldehyde (**9'**, grey, f) and deuterated cyanoformaldehyde (**8'**, blue, e).

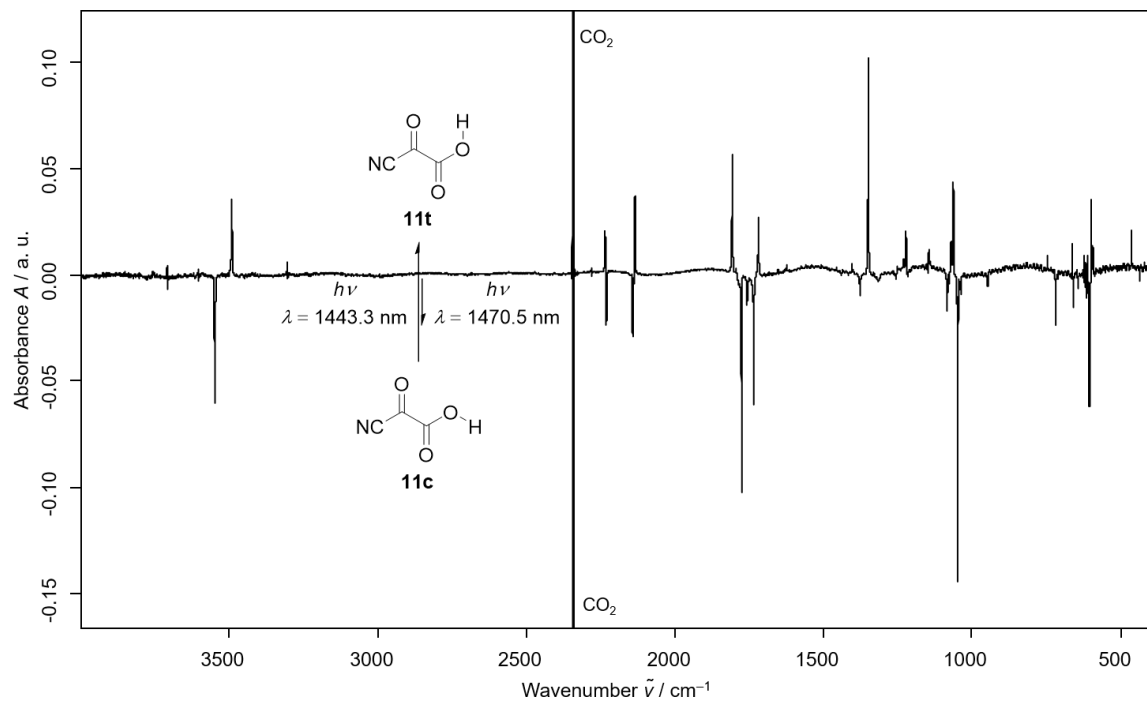


Figure S28: IR-difference spectra showing the interconversion of *cis* and *trans* **11** after NIR irradiation.

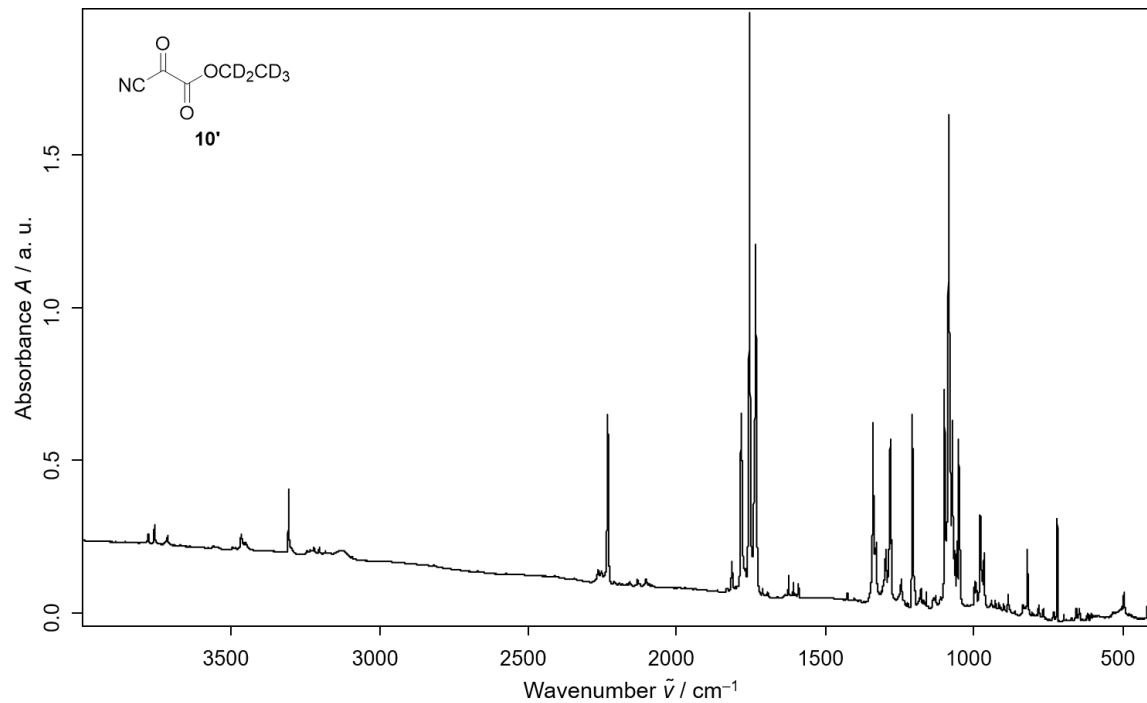


Figure S29: IR-spectrum of fully deuterated ethyl 2-cyano-2-oxoacetate precursor **10'**.

UV/Vis Spectrum

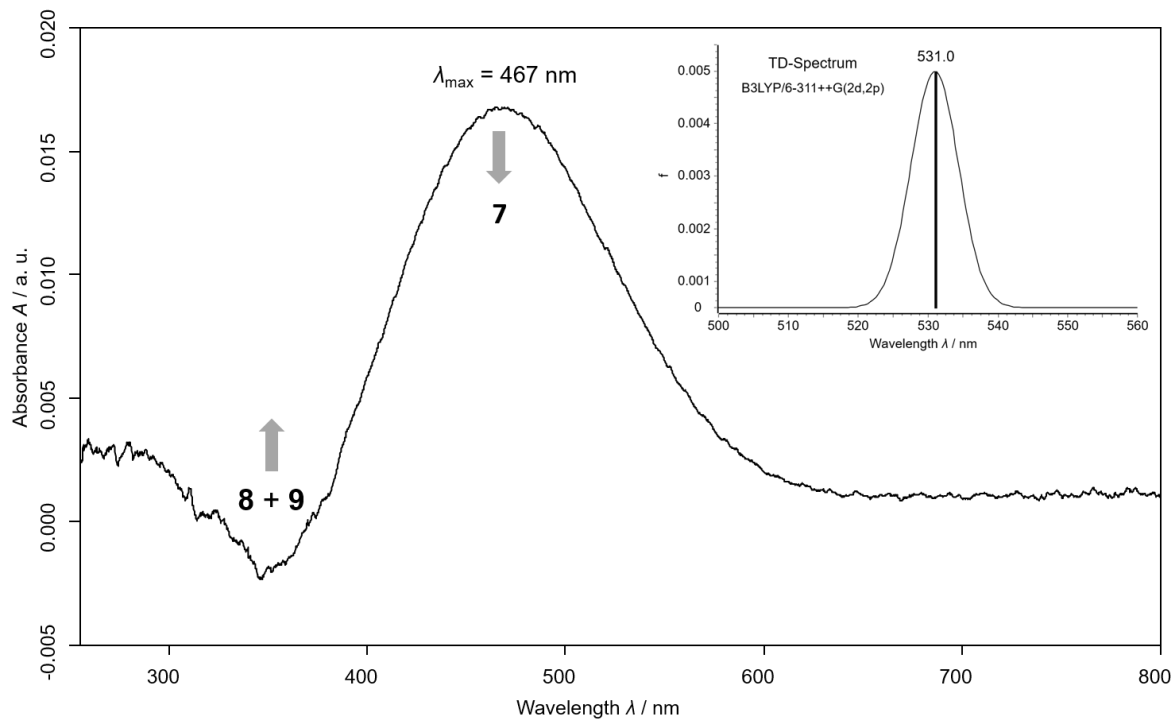


Figure S30: Experimental UV/Vis difference spectra between the spectra recorded after 18 min 520 nm irradiation and the spectrum recorded after 5 h pyrolysis of 2-cyano-2-oxo-acetic acid ethyl ester (**10**) at 900 °C. In this artificial spectra the signal of *trans*-cyanohydroxycarbene (**7t**) is pointing upwards although it is completely depleted after irradiation and the signal of cyano- and isocyanoformaldehyde **8** and **9** are pointing downwards although they increased after irradiation of the matrix. The TD-spectrum in the upper right corner was computed at B3LYP/6-311++G(2d,2p) level of theory.

Table S1: TD-DFT B3LYP/6-311++G(2d,2p) computed vertical excitation energies of *trans*-cyanohydroxycarbene **7t** and comparison with the recorded UV/Vis-spectrum.

excitation energy λ / nm	oscillator strength (f)	$\lambda_{\text{exp.}} / \text{nm}$	transition
531.0	0.0045	467	HOMO – LUMO
244.5	0.0011	n.o.	HOMO – LUMO+1
239.5	0.0115	n.o.	HOMO – LUMO+2

n.o. = not observed.

Table S2: TD-DFT B3LYP/6-311++G(2d,2p) computed vertical excitation energies of *cis* cyanohydroxycarbene **7c** and comparison with the recorded UV/Vis-spectrum.

excitation energy λ / nm	oscillator strength (f)	$\lambda_{\text{exp.}} / \text{nm}$	transition
535.5	0.0054	n.o.	HOMO – LUMO
249.5	0.0332	n.o.	HOMO – LUMO+1
242.5	0.0014	n.o.	HOMO – LUMO+2

n.o. = not observed.

Table S3: TD-DFT B3LYP/6-311++G(2d,2p) computed vertical excitation energy of cyanoformaldehyde **8** and comparison with the recorded UV/Vis-spectrum.

excitation energy λ / nm	oscillator strength (f)	$\lambda_{\text{exp.}} / \text{nm}$	transition
330.7	0.0005	350	HOMO – LUMO

Table S4: TD-DFT B3LYP/6-311++G(2d,2p) computed vertical excitation energy of isocyanoformaldehyde **9** and comparison with the recorded UV/Vis-spectrum.

excitation energy λ / nm	oscillator strength (f)	$\lambda_{\text{exp.}} / \text{nm}$	transition
282.4	0.0036	350	HOMO – LUMO

Spectroscopic Data

Table S5: Comparison of experimental vibrational frequencies of *trans*-cyanohydroxycarbene **7t** isolated in an argon matrix at 3 K and computed vibrational frequencies at the AE-CCSD(T)/cc-pCVQZ level of theory (unscaled).

Assignment	Sym.	$\tilde{\nu}_{\text{anharm.}} / \text{cm}^{-1}$	$I_{\text{abs}} / \text{km mol}^{-1}$	$\tilde{\nu}_{\text{harm}} / \text{cm}^{-1}$	$I_{\text{abs}} / \text{km mol}^{-1}$	$\tilde{\nu}_{\text{exp.}} / \text{cm}^{-1}$	I_{rel}
$\nu(\text{OH})$	a'	3571.0	145.1	3769.2	173.9	3511.8	s
$\nu(\text{CN})$	a'	2182.8	32.5	2221.6	33.5	2156.8	vw
$\nu(\text{CO}) + \delta(\text{COH})$	a'	1345.4	37.3	1387.8	27.3	1343.8	m
$\nu(\text{CO}) - \delta(\text{COH})$	a'	1297.1	252.2	1335.2	246.7	1287.9	vs
$\nu(\text{CC})$	a'	843.1	1.2	867.1	48.5	835.4	m
$\delta_{\text{oop}}(\text{COH})$	a''	845.5	77.7	858.8	76.1	829.8, 821.6	m
$\delta(\text{CCN}) + \delta(\text{OCC})$	a'	621.5	4.0	628.8	4.0	n. o.	
$\delta_{\text{oop}}(\text{CCN})$	a''	318.5	0.7	278.9	1.2	o. o. r.	
$\delta(\text{CCN}) - \delta(\text{OCC})$	a'	273.9	3.1	241.1	2.7	o. o. r.	

rel. experimental intensities (vw = very weak, w = weak, m = middle, s = strong, vs = very strong); n.o. = not observed; o. o. r. = out of range.

Table S6: Comparison of experimental vibrational frequencies of *cis*-cyanohydroxycarbene **7c** isolated in an argon matrix at 3 K and computed vibrational frequencies at the AE-CCSD(T)/cc-pCVQZ level of theory (unscaled).

Assignment	Sym.	$\tilde{\nu}_{\text{anharm.}} / \text{cm}^{-1}$	$I_{\text{abs}} / \text{km mol}^{-1}$	$\tilde{\nu}_{\text{harm}} / \text{cm}^{-1}$	$I_{\text{abs}} / \text{km mol}^{-1}$	$\tilde{\nu}_{\text{exp.}} / \text{cm}^{-1}$	I_{rel}
$\nu(\text{OH})$	a'	3397.7	15.4	3619.4	26.6	3365.4	w
$\nu(\text{CN})$	a'	2167.4	13.2	2209.2	27.1	n. o.	
$\nu(\text{CO}) + \delta(\text{COH})$	a'	1343.6	21.7	1383.7	13.6	1302.1	vw
$\nu(\text{CO}) - \delta(\text{COH})$	a'	1285.7	217.6	1327.7	227.0	1272.2	s
$\nu(\text{CC})$	a'	824.0	14.6	841.6	14.2	812.3	vw
$\delta_{\text{oop}}(\text{COH})$	a''	809.5	113.5	840.9	110.7	801.9	m
$\delta(\text{CCN}) + \delta(\text{OCC})$	a'	630.7	3.5	643.2	2.9	n. o.	
$\delta_{\text{oop}}(\text{CCN})$	a''	274.3	34.2	271.8	58.4	o. o. r.	
$\delta(\text{CCN}) - \delta(\text{OCC})$	a'	213.3	23.3	217.2	24.6	o. o. r.	

rel. experimental intensities (vw = very weak, w = weak, m = middle, s = strong, vs = very strong); n.o. = not observed; o. o. r. = out of range.

Table S7: Comparison of experimental vibrational frequencies of deuterated *trans*-cyanohydroxycarbene-*O-D* **7t'** isolated in an argon matrix at 3 K and computed vibrational frequencies at the AE-CCSD(T)/cc-pCVQZ level of theory (unscaled).

Assignment	Sym.	$\tilde{\nu}_{\text{anharm.}} / \text{cm}^{-1}$	$I_{\text{abs}} / \text{km mol}^{-1}$	$\tilde{\nu}_{\text{harm}} / \text{cm}^{-1}$	$I_{\text{abs}} / \text{km mol}^{-1}$	$\tilde{\nu}_{\text{exp.}} / \text{cm}^{-1}$	I_{rel}
$\nu(\text{OD})$	a'	2661.5	84.7	2744.8	93.5	2598.1	s
$\nu(\text{CN})$	a'	2188.4	33.6	2221.4	34.3	2166.4	m
$\nu(\text{CO})$	a'	1334.5	140.7	1357.9	176.2	1327.4	vs
$\delta(\text{COD})$	a'	1074.4	36.2	1086.5	35.3	1050.6	m
$\nu(\text{CC})$	a'	802.3	56.2	807.7	56.0	780.8	m
$\delta_{\text{oop}}(\text{COD})$	a''	706.8	39.5	660.2	42.9	642.4	w
$\delta(\text{CCN}) + \delta(\text{OCC})$	a'	614.4	4.2	622.0	5.4	n. o.	
$\delta_{\text{oop}}(\text{CCN})$	a''	342.6	3.7	266.2	1.0	o. o. r.	
$\delta(\text{CCN}) - \delta(\text{OCC})$	a'	269.7	3.3	236.0	2.4	o. o. r.	

rel. experimental intensities (vw = very weak, w = weak, m = middle, s = strong, vs = very strong); n.o. = not observed; o. o. r. = out of range.

Table S8: Comparison of experimental vibrational frequencies of deuterated *cis*-cyanohydroxycarbene-*O-D* **7c'** isolated in an argon matrix at 3 K and computed vibrational frequencies at the AE-CCSD(T)/cc-pCVQZ level of theory (unscaled).

Assignment	Sym.	$\tilde{\nu}_{\text{anharm.}} / \text{cm}^{-1}$	$I_{\text{abs}} / \text{km mol}^{-1}$	$\tilde{\nu}_{\text{harm}} / \text{cm}^{-1}$	$I_{\text{abs}} / \text{km mol}^{-1}$	$\tilde{\nu}_{\text{exp.}} / \text{cm}^{-1}$	I_{rel}
$\nu(\text{OD})$	a'	2571.0	12.2	2635.6	14.0	2498.7	m
$\nu(\text{CN})$	a'	2176.1	27.5	2209.1	27.7	2150.7	w
$\nu(\text{CO})$	a'	1328.2	129.8	1359.8	142.7	1328.8	m
$\delta(\text{COD})$	a'	1052.0	55.8	1058.4	53.3	1021.2	s
$\nu(\text{CC})$	a'	796.5	12.0	810.5	11.3	n. o.	
$\delta_{\text{oop}}(\text{COD})$	a''	691.2	37.3	673.0	35.4	649.0	s
$\delta(\text{CCN}) + \delta(\text{OCC})$	a'	619.8	3.7	624.0	3.3	n. o.	
$\delta_{\text{oop}}(\text{CCN})$	a''	286.1	42.0	263.9	50.6	o. o. r.	
$\delta(\text{CCN}) - \delta(\text{OCC})$	a'	209.4	21.5	210.5	23.5	o. o. r.	

rel. experimental intensities (vw = very weak, w = weak, m = middle, s = strong, vs = very strong); n.o. = not observed; o. o. r. = out of range.

Table S9: Comparison of experimental vibrational frequencies of *trans*-2-cyano-2-oxo acetic acid **11t** isolated in an argon matrix at 3 K and computed vibrational frequencies at the AE-CCSD(T)/cc-pCVQZ level of theory (unscaled).

Assignment	Sym.	$\tilde{\nu}_{\text{anharm.}} / \text{cm}^{-1}$	$I_{\text{abs}} / \text{km mol}^{-1}$	$\tilde{\nu}_{\text{harm}} / \text{cm}^{-1}$	$I_{\text{abs}} / \text{km mol}^{-1}$	$\tilde{\nu}_{\text{exp.}} / \text{cm}^{-1}$	I_{rel}
$\nu(\text{OH})$	a'	3688.0	107.2	3502.0	108.1	3491.7	m
$\nu(\text{CN})$	a'	2331.0	55.1	2300.7	88.6	2236.0	m
$\nu(\text{CO})$	a'	1846.0	222.5	1812.4	441.3	1808.2	s
$\nu(\text{CO})$	a'	1760.9	121.6	1735.0	258.0	1719.5	m
$\delta(\text{COH}), \nu(\text{CC})$	a'	1372.3	314.0	1336.9	692.1	1348.9	vs
$\delta(\text{COH}), \nu(\text{CC})$	a'	1221.1	51.9	1156.2	279.7	1223.7	m
$\nu(\text{CC}), \nu(\text{CO})$	a'	1086.1	219.7	1058.6	652.1	1063.8	s
$\delta(\text{OCC})$	a''	826.5	0.6	739.7	34.9	n. o.	
$\nu(\text{CC})$	a'	751.7	7.3	655.6	37.1	746.2	vw
$\delta(\text{CCN}) + \delta(\text{OCC})$	a'	661.0	6.9	502.2	5.1	663.2	w
$\gamma(\text{OCOH})$	a''	647.2	91.0	417.1	18.6	598.6	m
$\gamma(\text{OCCO})$	a'	510.6	1.1	281.7	519.2	n. o.	
$\gamma(\text{OCCC})$	a''	476.4	25.5	144.1	64.9	464.1	m
$\nu(\text{CC})$	a'	427.8	3.3	815.1	1.4	n. o.	
$\gamma(\text{OCCO})$	a'	286.9	41.3	616.1	564.6	o. o. r.	
$\delta_{\text{oop}}(\text{CCN})$	a''	248.7	25.8	468.6	220.9	o. o. r.	
$\delta(\text{CCN}) - \delta(\text{OCC})$	a'	145.9	2.4	242.7	411.3	o. o. r.	
$\gamma(\text{OCCO})$	a''	75.1	0.9	73.1	51.2	o. o. r.	

rel. experimental intensities (vw = very weak, w = weak, m = middle, s = strong, vs = very strong); n.o. = not observed; o. o. r. = out of range.

Table S10: Comparison of experimental vibrational frequencies of *cis*-2-cyano-2-oxo acetic acid **11c** isolated in an argon matrix at 3 K and computed vibrational frequencies at the AE-CCSD(T)/cc-pCVQZ level of theory (unscaled).

Assignment	Sym.	$\tilde{\nu}_{\text{anharm.}} / \text{cm}^{-1}$	$I_{\text{abs}} / \text{km mol}^{-1}$	$\tilde{\nu}_{\text{harm}} / \text{cm}^{-1}$	$I_{\text{abs}} / \text{km mol}^{-1}$	$\tilde{\nu}_{\text{exp.}} / \text{cm}^{-1}$	I_{rel}
$\nu(\text{OH})$	a'	3753.2	116.0	3564.7	113.1	3549.3	m
$\nu(\text{CN})$	a'	2327.5	47.6	2295.4	74.4	2231.7	w
$\nu(\text{CO})$	a'	1808.9	288.8	1778.8	680.5	1776.3	s
$\nu(\text{CO})$	a'	1787.6	110.7	1761.6	158.9	1735.0	m
$\delta(\text{COH}), \nu(\text{CC})$	a'	1392.5	18.7	1354.4	47.9	1376.9	vw
$\delta(\text{COH}), \nu(\text{CC})$	a'	1203.7	67.8	1144.1	110.4	n. o.	
$\nu(\text{CC}), \nu(\text{CO})$	a'	1062.5	312.9	1035.6	726.0	1048.7	vs
$\delta(\text{OCC})$	a''	826.9	2.0	713.4	278.6	n. o.	
$\nu(\text{CC})$	a'	722.2	63.1	651.0	126.6	719.6	w
$\delta(\text{CCN}) + \delta(\text{OCC})$	a'	655.7	24.5	501.0	20.5	658.6	vw
$\gamma(\text{OCOH})$	a''	636.9	139.5	432.8	66.9	605.4	m
$\gamma(\text{OCCO})$	a'	495.5	2.4	279.6	201.6	n. o.	
$\gamma(\text{OCOH})$	a''	453.8	3.9	149.8	13.9	n. o.	
$\nu(\text{CC})$	a'	434.6	14.8	814.1	6.7	435.1	vw
$\gamma(\text{OCCO})$	a'	280.1	16.3	606.4	865.1	o. o. r.	
$\delta_{\text{oop}}(\text{CCN})$	a''	240.3	12.8	440.0	52.1	o. o. r.	
$\delta(\text{CCN}) - \delta(\text{OCC})$	a'	148.4	0.6	239.1	192.9	o. o. r.	
$\gamma(\text{OCCO})$	a''	37.7	1.4	28.0	230.5	o. o. r.	

rel. experimental intensities (vw = very weak, w = weak, m = middle, s = strong, vs = very strong); n.o. = not observed; o. o. r. = out of range.

Tunnelling Kinetic Analysis

Tunnelling kinetics of matrix-isolated cyanohydroxycarbene **7t** was evaluated by recording infrared spectra in regular intervals (8 h or one spectrum per day) for a period of 47 days. For the determination of the tunnelling half-life only the absorbance A of the strongest IR-signal, appearing at 1287.9 cm^{-1} , as depicted in Figure 3, was evaluated after a first order kinetic model. After a direct exponential fit the rate constant k_1 and corresponding tunnelling half-life τ was observed.

$$A = A_0 + A_1 \cdot \exp(-k_1 \cdot t)$$

All nonlinear fits were determined using the ExpDec1 model implemented in OriginPro 2017 9.4.0 (OriginLab Corporation, 2016; <http://www.originlab.com>).

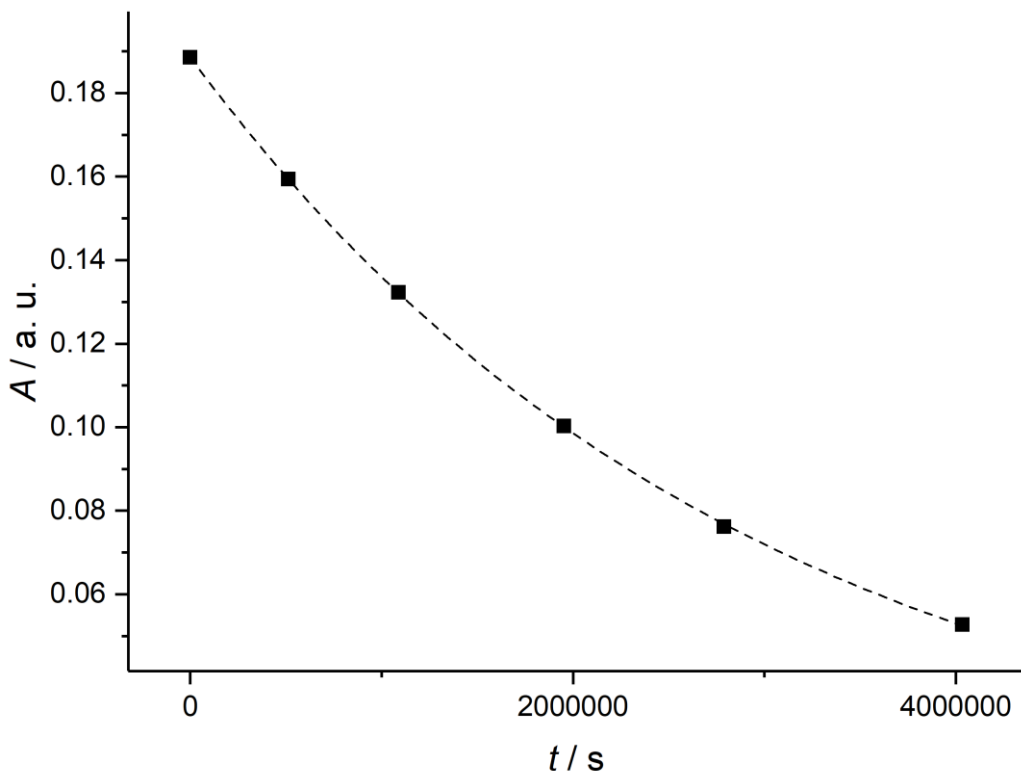


Figure S31: Kinetic evaluation of the IR band at 1287.9 cm^{-1} as represented in Figure 3 of *trans*-cyanohydroxycarbene **7t** in Ar (3 K).

Table S11: Kinetic fit-parameters of Figure S31.

	Value	Standard Error
A_0	0.00644	0.00221
A_1	0.18216	0.00205
k_1 / s^{-1}	$3.41 \cdot 10^{-7}$	$7.49 \cdot 10^{-9}$
τ / d	23.5	0.5

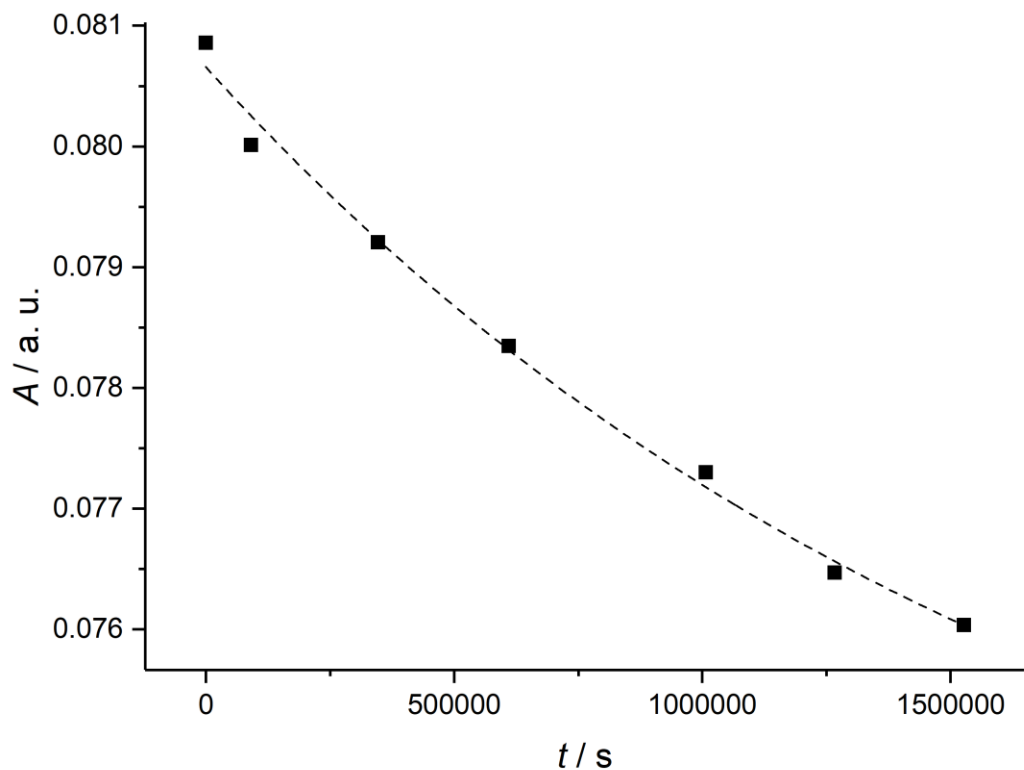


Figure S32: Kinetic evaluation of the IR band at 1287.9 cm^{-1} as represented in Figure 3 of *trans*-cyanohydroxycarbene **7t** in Ar (12 K).

Table S12: Kinetic fit-parameters of Figure S32.

	Value	Standard Error
A_0	0.07276	0.00190
A_1	0.00790	0.00184
k_1 / s^{-1}	$5.76 \cdot 10^{-7}$	$2.08 \cdot 10^{-7}$
τ / d	20.1	7.3

WKB Tunnelling Computations

For the estimation of the tunnelling rate, we mapped out the intrinsic reaction path starting from TS_1 at MP2/cc-pVTZ level of theory. In order to do so, we employed the Hessian-based predictor-corrector integrator as implemented in the Gaussian09 electronic structure package. Zero-point vibrational corrections for all modes orthogonal to the reaction path were added to the reaction profile. Tunnelling probabilities were calculated by numerically integrating the barrier penetration integral and evaluating the WKB equation. Based on the inspection of the projected frequencies along the minimum energy path, we used vibrational mode #4 (1332 cm^{-1}) as the reactive mode for tunnelling computations in the reaction of $7\mathbf{t} \rightarrow 8$.

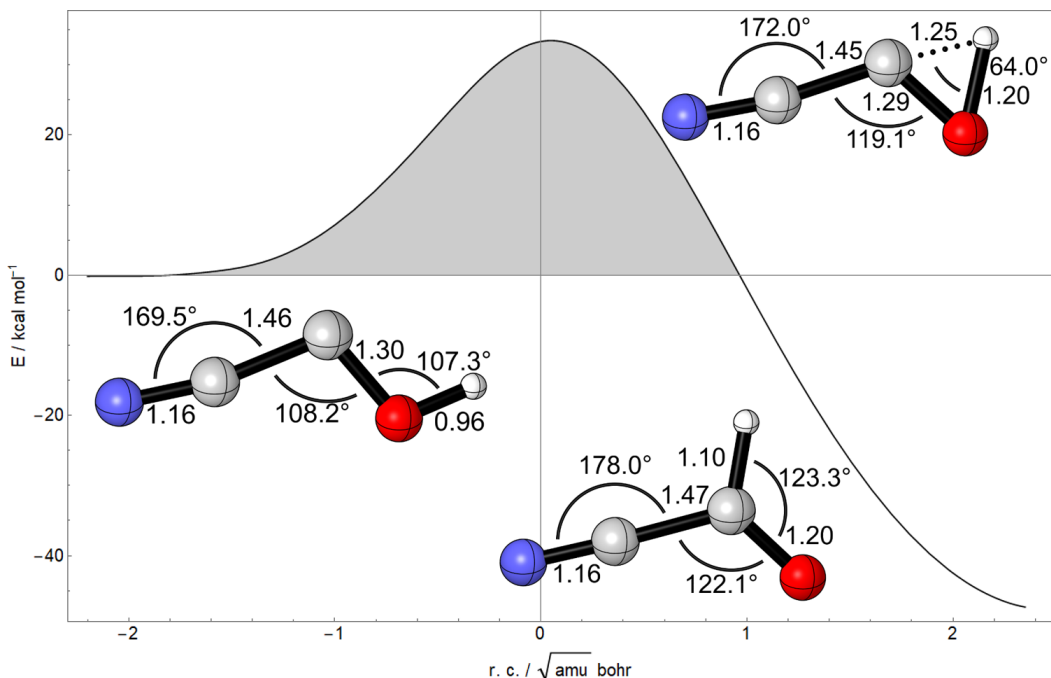


Figure S33: Computed reaction path for the [1,2]H-tunnelling reaction of *trans*-cyanohydroxycarbene $7\mathbf{t}$ to cyanoformaldehyde 8 at AE-CCSD(T)/cc-pCVQZ//MP2/cc-pVTZ level of theory.

Table S13: WKB-tunnelling analysis for the reaction of *trans*-cyanohydroxycarbene $7\mathbf{t}$ to cyanoformaldehyde 8 .

Tunnelling parameters	Cyanohydroxycarbene	Cyanohydroxycarbene-O-D
Collision energy ($\varepsilon / \text{kcal mol}^{-1}$)	1.9	1.5
Collision frequency ($\omega_0 / \text{cm}^{-1}$)	1332	1083
Barrier (kcal mol^{-1})	33.4	34.4
Effective barrier (kcal mol^{-1})	35.4	35.9
Turning points [(s1, s2), a.u.]	-1.81, 0.96	-2.65, 1.35
Barrier penetration integral (θ)	23.7	33.1
WKB transmission probability (κ_{WKB})	$2.62 \cdot 10^{-19}$	$1.72 \cdot 10^{-27}$
WKB half-life ($v = 0; \tau_{\text{WKB}}$)	77 d	$3.9 \cdot 10^7$ y
WKB half-life ($v = 1; \tau_{\text{WKB}}$)	2.5 d	$8.4 \cdot 10^5$ y
WKB half-life ($v = 2; \tau_{\text{WKB}}$)	2.7 h	$2.7 \cdot 10^4$ y

^aThe effective barrier for tunnelling differs from the values depicted in Figure S33 because one specific frequency corresponding to the reaction mode has been projected out at all points along the IRP.

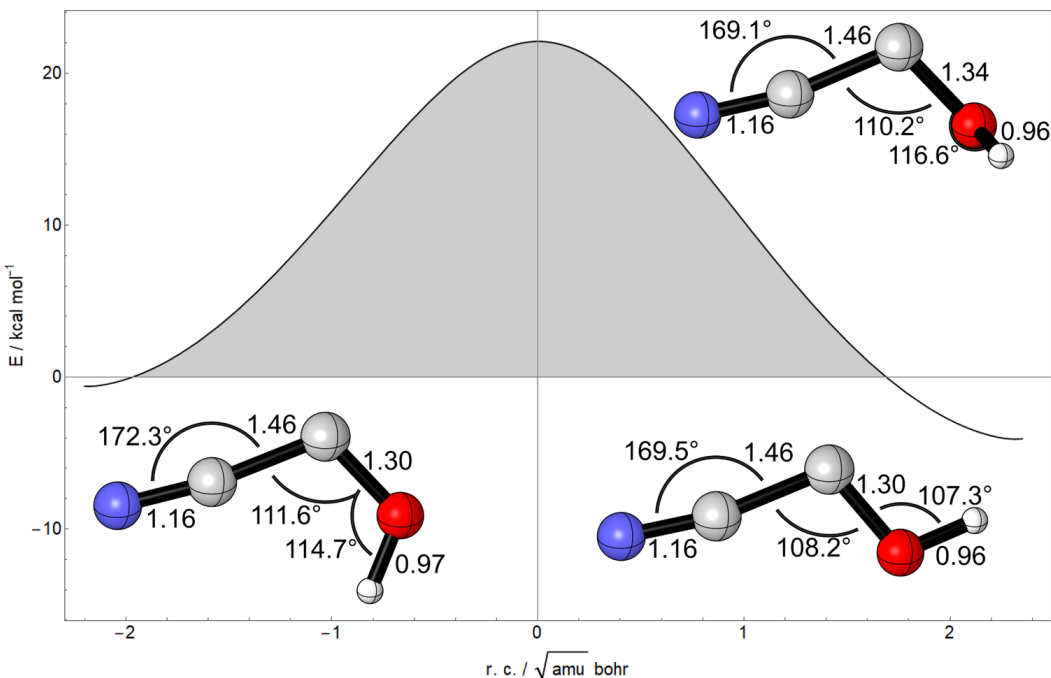


Figure S34: Computed reaction path for the H-tunnelling reaction of *cis*-cyanohydroxycarbene **7c** to *trans*-cyanohydroxycarbene **7t** at AE-CCSD(T)/cc-pCVQZ//MP2/cc-pVTZ level of theory.

Table S14: WKB-tunnelling analysis for the reaction of *cis*-cyanohydroxycarbene **7c** to *trans*-cyanohydroxycarbene **7t**.

Tunnelling parameters	Cyanohydroxycarbene
Collision energy (ε / kcal mol ⁻¹)	1.0
Collision frequency (ω_0 / cm ⁻¹)	695
Barrier (kcal mol ⁻¹)	22.1
Effective barrier (kcal mol ⁻¹)	23.1
Turning points [(s ₁ , s ₂), a.u.]	-1.97, 1.69
Barrier penetration integral (θ)	28.15
WKB transmission probability (κ_{WKB})	$3.53 \cdot 10^{-23}$
WKB half-life ($v = 0$; τ_{WKB})	$2.9 \cdot 10^4$ y
WKB half-life ($v = 1$; τ_{WKB})	438 y
WKB half-life ($v = 2$; τ_{WKB})	28 y

^aThe effective barrier for tunnelling differs from the values depicted in Figure S34 because one specific frequency corresponding to the reaction mode has been projected out at all points along the IRP.

Polyrate Tunnelling Computations

Table S15: Computed reaction rates in s^{-1} for the reaction of *trans*-cyanohydroxycarbene **7t** to cyanoformaldehyde **8** with polyrate at different temperatures.

T / K	TST	CVT	CVT/ZCT	CVT/SCT
35	$4.34 \cdot 10^{-198}$	$8.11 \cdot 10^{-281}$	$4.91 \cdot 10^{-11}$	$5.47 \cdot 10^{-9}$
40	$7.03 \cdot 10^{-172}$	$2.32 \cdot 10^{-244}$	$5.25 \cdot 10^{-11}$	$5.85 \cdot 10^{-9}$
45	$1.73 \cdot 10^{-151}$	$5.29 \cdot 10^{-216}$	$5.49 \cdot 10^{-11}$	$6.12 \cdot 10^{-9}$
50	$3.60 \cdot 10^{-135}$	$2.59 \cdot 10^{-193}$	$5.65 \cdot 10^{-11}$	$6.30 \cdot 10^{-9}$
60	$1.11 \cdot 10^{-110}$	$2.86 \cdot 10^{-159}$	$5.81 \cdot 10^{-11}$	$6.48 \cdot 10^{-9}$
70	$3.51 \cdot 10^{-93}$	$5.99 \cdot 10^{-135}$	$5.84 \cdot 10^{-11}$	$6.51 \cdot 10^{-9}$
80	$4.80 \cdot 10^{-80}$	$1.05 \cdot 10^{-116}$	$5.80 \cdot 10^{-11}$	$6.46 \cdot 10^{-9}$
90	$8.02 \cdot 10^{-70}$	$1.65 \cdot 10^{-102}$	$5.71 \cdot 10^{-11}$	$6.35 \cdot 10^{-9}$
100	$1.22 \cdot 10^{-61}$	$3.74 \cdot 10^{-91}$	$5.62 \cdot 10^{-11}$	$6.21 \cdot 10^{-9}$
110	$6.14 \cdot 10^{-55}$	$7.35 \cdot 10^{-82}$	$5.56 \cdot 10^{-11}$	$6.06 \cdot 10^{-9}$
120	$2.38 \cdot 10^{-49}$	$4.09 \cdot 10^{-74}$	$5.55 \cdot 10^{-11}$	$5.92 \cdot 10^{-9}$
130	$1.28 \cdot 10^{-44}$	$1.46 \cdot 10^{-67}$	$5.62 \cdot 10^{-11}$	$5.78 \cdot 10^{-9}$
140	$1.46 \cdot 10^{-40}$	$6.07 \cdot 10^{-62}$	$5.81 \cdot 10^{-11}$	$5.67 \cdot 10^{-9}$
150	$4.84 \cdot 10^{-37}$	$4.49 \cdot 10^{-57}$	$6.14 \cdot 10^{-11}$	$5.59 \cdot 10^{-9}$
160	$5.84 \cdot 10^{-34}$	$8.17 \cdot 10^{-53}$	$6.65 \cdot 10^{-11}$	$5.54 \cdot 10^{-9}$
170	$3.07 \cdot 10^{-31}$	$4.69 \cdot 10^{-49}$	$7.39 \cdot 10^{-11}$	$5.52 \cdot 10^{-9}$
180	$8.09 \cdot 10^{-29}$	$1.03 \cdot 10^{-45}$	$8.43 \cdot 10^{-11}$	$5.54 \cdot 10^{-9}$
190	$1.19 \cdot 10^{-26}$	$1.01 \cdot 10^{-42}$	$9.86 \cdot 10^{-11}$	$5.62 \cdot 10^{-9}$
200	$1.07 \cdot 10^{-24}$	$4.93 \cdot 10^{-40}$	$1.18 \cdot 10^{-10}$	$5.74 \cdot 10^{-9}$
220	$2.53 \cdot 10^{-21}$	$2.19 \cdot 10^{-35}$	$1.82 \cdot 10^{-10}$	$6.20 \cdot 10^{-9}$
240	$1.66 \cdot 10^{-18}$	$1.63 \cdot 10^{-31}$	$3.07 \cdot 10^{-10}$	$7.03 \cdot 10^{-9}$
260	$4.05 \cdot 10^{-16}$	$3.08 \cdot 10^{-28}$	$5.60 \cdot 10^{-10}$	$8.50 \cdot 10^{-9}$
280	$4.54 \cdot 10^{-14}$	$1.98 \cdot 10^{-25}$	$1.11 \cdot 10^{-09}$	$1.12 \cdot 10^{-8}$

Table S16: Computed reaction rates in s^{-1} for the reaction of deuterated *trans*-cyanohydroxycarbene **7t'** to deuterated cyanoformaldehyde with polyrate at different temperatures.

T / K	TST	CVT	CVT/ZCT	CVT/SCT
30	$1.96 \cdot 10^{-240}$	$5.12 \cdot 10^{-291}$	$1.44 \cdot 10^{-19}$	$9.64 \cdot 10^{-17}$
35	$1.94 \cdot 10^{-204}$	$6.26 \cdot 10^{-248}$	$1.66 \cdot 10^{-19}$	$1.11 \cdot 10^{-16}$
40	$1.97 \cdot 10^{-177}$	$1.31 \cdot 10^{-215}$	$1.83 \cdot 10^{-19}$	$1.23 \cdot 10^{-16}$
45	$2.01 \cdot 10^{-156}$	$1.83 \cdot 10^{-190}$	$1.97 \cdot 10^{-19}$	$1.32 \cdot 10^{-16}$
50	$1.31 \cdot 10^{-139}$	$2.40 \cdot 10^{-170}$	$2.08 \cdot 10^{-19}$	$1.40 \cdot 10^{-16}$
60	$2.22 \cdot 10^{-114}$	$3.68 \cdot 10^{-140}$	$2.25 \cdot 10^{-19}$	$1.51 \cdot 10^{-16}$
70	$2.40 \cdot 10^{-96}$	$1.36 \cdot 10^{-118}$	$2.36 \cdot 10^{-19}$	$1.58 \cdot 10^{-16}$
80	$8.18 \cdot 10^{-83}$	$2.06 \cdot 10^{-102}$	$2.45 \cdot 10^{-19}$	$1.63 \cdot 10^{-16}$
90	$2.79 \cdot 10^{-72}$	$7.99 \cdot 10^{-90}$	$2.54 \cdot 10^{-19}$	$1.66 \cdot 10^{-16}$
100	$7.54 \cdot 10^{-64}$	$9.46 \cdot 10^{-80}$	$2.67 \cdot 10^{-19}$	$1.69 \cdot 10^{-16}$
110	$6.04 \cdot 10^{-57}$	$1.66 \cdot 10^{-71}$	$2.92 \cdot 10^{-19}$	$1.71 \cdot 10^{-16}$
120	$3.45 \cdot 10^{-51}$	$1.23 \cdot 10^{-64}$	$3.35 \cdot 10^{-19}$	$1.74 \cdot 10^{-16}$
130	$2.58 \cdot 10^{-46}$	$8.04 \cdot 10^{-59}$	$4.08 \cdot 10^{-19}$	$1.79 \cdot 10^{-16}$
140	$3.92 \cdot 10^{-42}$	$7.76 \cdot 10^{-54}$	$5.31 \cdot 10^{-19}$	$1.86 \cdot 10^{-16}$
150	$1.66 \cdot 10^{-38}$	$1.62 \cdot 10^{-49}$	$7.36 \cdot 10^{-19}$	$1.96 \cdot 10^{-16}$
160	$2.48 \cdot 10^{-35}$	$9.80 \cdot 10^{-46}$	$1.08 \cdot 10^{-18}$	$2.10 \cdot 10^{-16}$
170	$1.58 \cdot 10^{-32}$	$2.13 \cdot 10^{-42}$	$1.68 \cdot 10^{-18}$	$2.33 \cdot 10^{-16}$
180	$4.93 \cdot 10^{-30}$	$1.97 \cdot 10^{-39}$	$2.76 \cdot 10^{-18}$	$2.66 \cdot 10^{-16}$
190	$8.42 \cdot 10^{-28}$	$8.86 \cdot 10^{-37}$	$4.83 \cdot 10^{-18}$	$3.17 \cdot 10^{-16}$
200	$8.64 \cdot 10^{-26}$	$2.17 \cdot 10^{-34}$	$8.97 \cdot 10^{-18}$	$4.00 \cdot 10^{-16}$
220	$2.59 \cdot 10^{-22}$	$2.89 \cdot 10^{-30}$	$3.73 \cdot 10^{-17}$	$7.86 \cdot 10^{-16}$
240	$2.07 \cdot 10^{-19}$	$7.93 \cdot 10^{-27}$	$2.00 \cdot 10^{-16}$	$2.20 \cdot 10^{-15}$
260	$5.95 \cdot 10^{-17}$	$6.43 \cdot 10^{-24}$	$1.37 \cdot 10^{-15}$	$8.93 \cdot 10^{-15}$
280	$7.66 \cdot 10^{-15}$	$2.00 \cdot 10^{-21}$	$1.19 \cdot 10^{-14}$	$5.00 \cdot 10^{-14}$

Instanton Tunnelling Computations

Table S17: Computed instanton tunnelling rates and tunnelling half-lives for the reaction of *trans*-cyanohydroxycarbene **7t** and its *O*-deuterated isotopologue **7t'** to the corresponding cyanoformaldehyde **8** and **8'** isotopologues with DL-FIND included in ChemShell.

Images	T / K	7t ln(k / s ⁻¹)	7t' (O-D) ln(k / s ⁻¹)	7t τ / d	7t' (O-D) τ / d	KIE
32	450	-4.11	-8.74	0.0	0.1	103
32	400	-7.67	-17.21	0.0	238.9	1383
32	300	-12.82	-31.24	3.0	2.96 · 10 ⁸	1.00 · 10 ⁸
32	250	-14.21	-35.63	11.9	2.39 · 10 ¹⁰	2.01 · 10 ⁹
32	200	-14.95	-38.00	24.9	2.56 · 10 ¹¹	1.03 · 10 ¹⁰
32	180	-15.11	-39.64	29.2	1.32 · 10 ¹²	4.53 · 10 ¹⁰
32	160	-15.22	-39.97	32.6	1.84 · 10 ¹²	5.63 · 10 ¹⁰
32	140	-15.28	-40.18	34.9	2.26 · 10 ¹²	6.49 · 10 ¹⁰
64	120	-15.37	-40.35	37.8	2.68 · 10 ¹²	7.08 · 10 ¹⁰
64	100	-15.39	-40.44	38.7	2.92 · 10 ¹²	7.55 · 10 ¹⁰
64	90	-15.39	-40.47	38.9	3.01 · 10 ¹²	7.75 · 10 ¹⁰
128	60	-15.42	-40.55	39.9	3.28 · 10 ¹²	8.24 · 10 ¹⁰

NBO Analysis

All natural bond orbitals (NBOs) were computed with the HF/6-311++G(2d,2p) level of theory based on AE-CCSD(T)/cc-pCVQZ optimized structures.

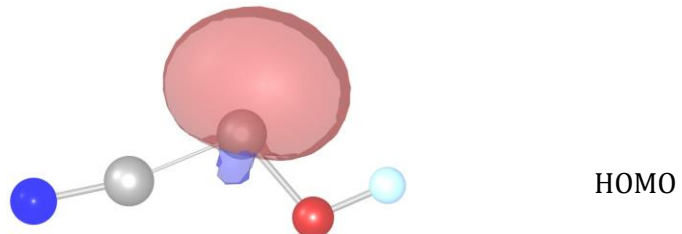


Figure S35: The HOMO NBO of *trans*-cyanohydroxycarbene **7t** is a σ_{out} type orbital that reflects the nucleophilic character of the carbene. HOMO = highest occupied molecular orbital.

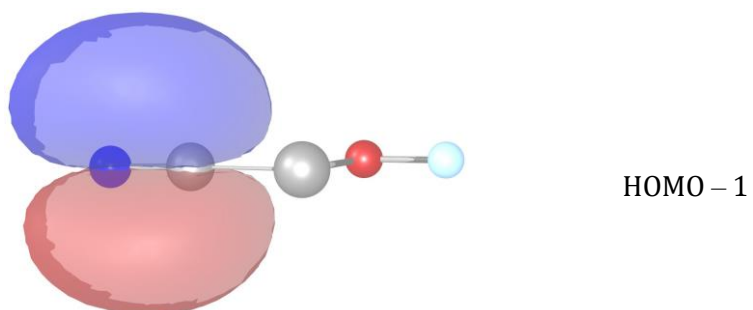


Figure S36: The π bond of the cyano-group in *trans*-cyanohydroxycarbene **7t** is represented in the HOMO – 1 NBO. HOMO = highest occupied molecular orbital

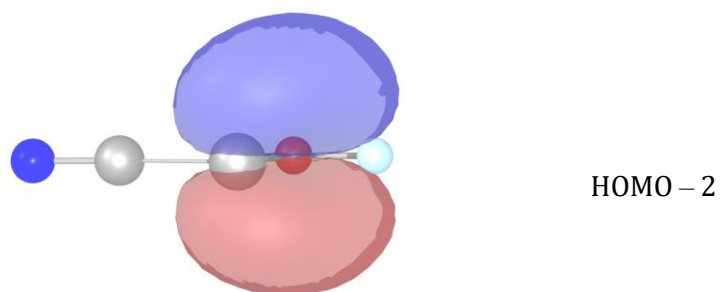


Figure S37: The HOMO – 2 NBO of *trans*-cyanohydroxycarbene **7t** is involved in the π delocalisation that is responsible for the shortened C–O bond. The orbital arises from electron donation from the oxygen p-orbital to the empty p-orbital of the carbene centre (see LUMO NBO, Figure S38). HOMO = highest occupied molecular orbital; LUMO = lowest unoccupied molecular orbital.

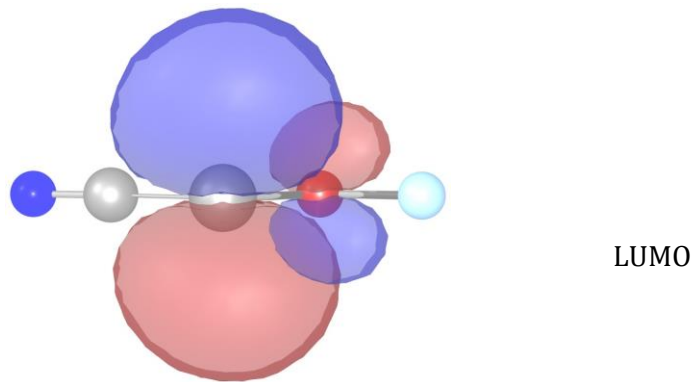


Figure S38: The LUMO NBO of *trans*-cyanohydroxycarbene **7t** shows the empty p-orbital of the carbene centre. LUMO = lowest unoccupied molecular orbital.

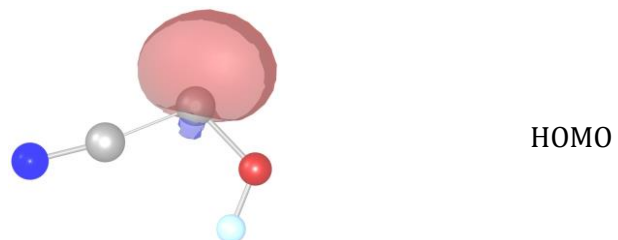


Figure S39: The HOMO NBO of *cis*-cyanohydroxycarbene **7c** is a σ_{out} type orbital that reflects the nucleophilic character of the carbene. HOMO = highest occupied molecular orbital.

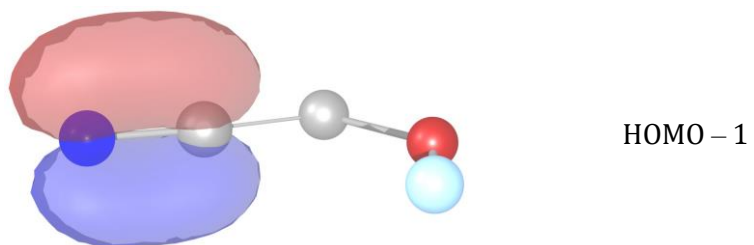


Figure S40: The π bond of the cyano-group in *cis*-cyanohydroxycarbene **7c** is represented in the HOMO – 1 NBO. HOMO = highest occupied molecular orbital

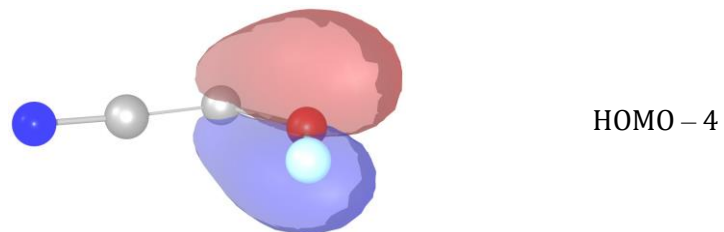


Figure S41: The HOMO – 4 NBO of *cis*-cyanohydroxycarbene **7c** is involved in the π delocalisation that is responsible for the shortened C–O bond. The orbital arises from electron donation from the oxygen p-orbital to the empty p-orbital of the carbene centre (see LUMO NBO, Figure S42). HOMO = highest occupied molecular orbital; LUMO = lowest unoccupied molecular orbital.

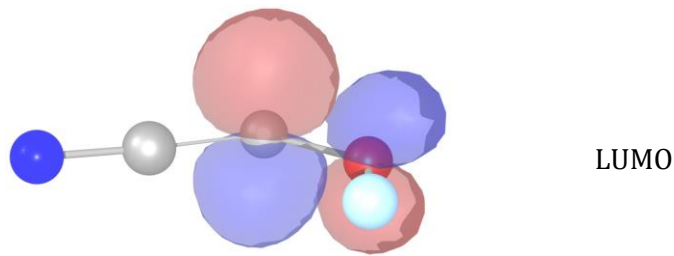


Figure S42: The LUMO NBO of *cis*-cyanohydroxycarbene **7c** shows the empty p-orbital of the carbene centre. LUMO = lowest unoccupied molecular orbital.

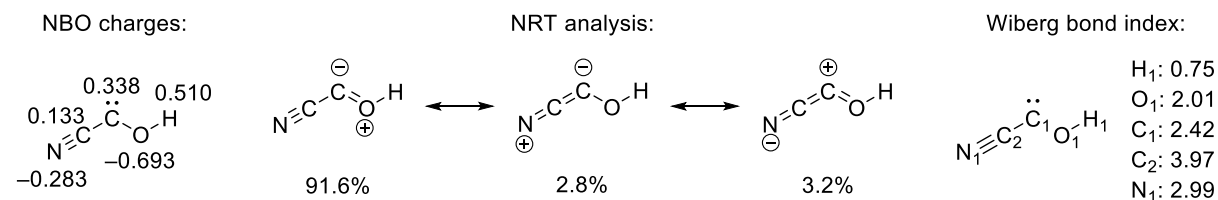


Figure S43: NBO analysis of *trans*-cyanohydroxycarbene **7t** at HF/6-311++G(2d,2p) level of theory based on the AE-CCSD(T)/cc-pCVQZ optimized geometry of **7t**.

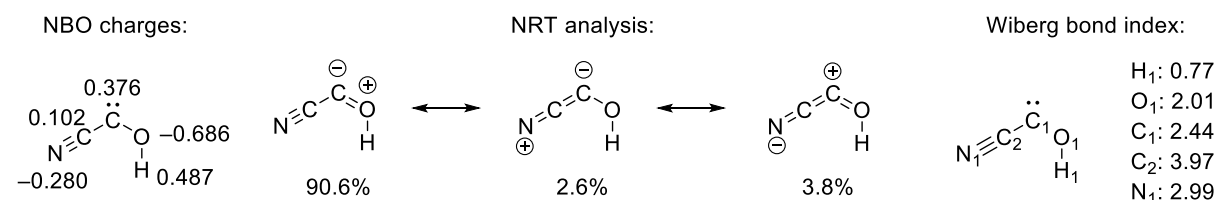


Figure S44: NBO analysis of *cis*-cyanohydroxycarbene **7c** at HF/6-311++G(2d,2p) level of theory based on the AE-CCSD(T)/cc-pCVQZ optimized geometry of **7c**.

Potential Energy Surfaces and Cartesian Coordinates for Selected Structures

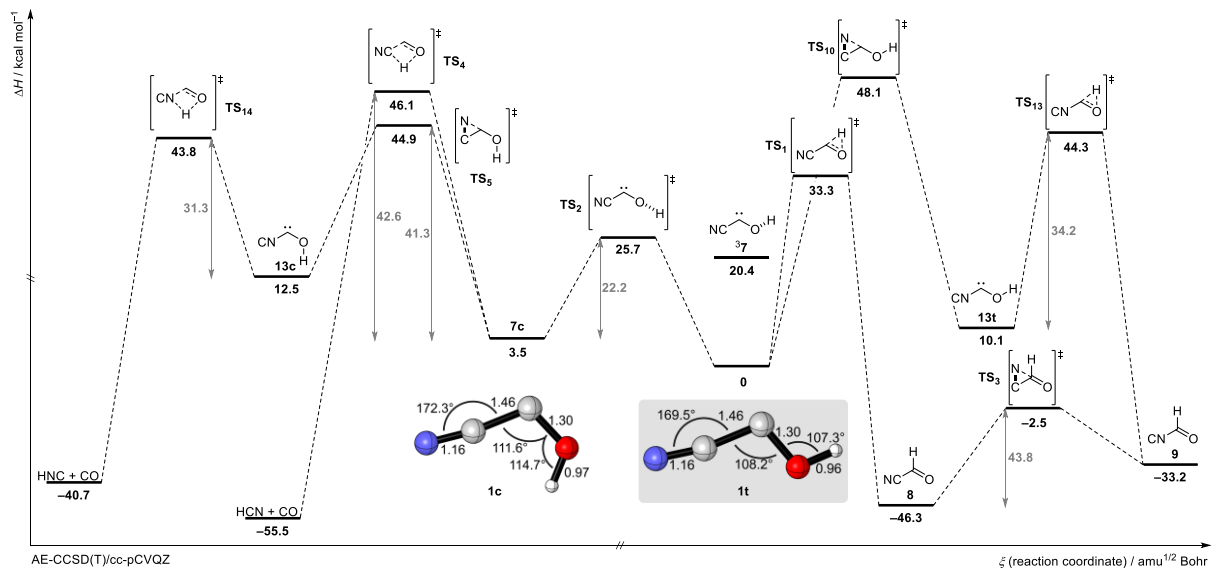


Figure S45: Computed potential energy surface (PES) around cyanohydroxycarbene **7** including the zero-point vibrational energy (ZPVE) at the AE-CCSD(T)/cc-pCVQZ level of theory.

AE-CCSD(T)/cc-pCVQZ optimized structures (distances in bohr), electronic energies and zero-point vibrational energies (ZPVE).

trans-Cyanohydroxycarbene **7t** (C_s)

H	-4.50225890	0.02934904	0.00000000
O	-2.82795780	-0.69307830	0.00000000
C	-1.22234700	1.17815571	0.00000000
C	1.32098024	0.12575931	0.00000000
N	3.46972628	-0.32784450	0.00000000

$$E = -206.6344591 \text{ au}$$

$$\text{ZPVE} = 16.5667 \text{ kcal mol}^{-1}$$

cis-Cyanohydroxycarbene **7c** (C_s)

H	-2.25197647	2.28627561	0.00000000
O	-2.93635602	0.58160936	0.00000000
C	-1.24488755	-1.20660161	0.00000000
C	1.32039390	-0.17858881	0.00000000
N	3.45140545	0.35815901	0.00000000

$$E = -206.6283019 \text{ au}$$

$$\text{ZPVE} = 16.2323 \text{ kcal mol}^{-1}$$

Cyanoformaldehyde **8** (C_s)

H	1.67546923	2.91593956	0.00000000
C	1.32566500	0.87508967	0.00000000
O	2.98428975	-0.67460260	0.00000000
C	-1.36374569	0.15984507	0.00000000
N	-3.49673732	-0.32619715	0.00000000

E = -206.7081683 au

ZPVE = 16.5174 kcal mol⁻¹

Isocyanoformaldehyde **9** (C_s)

H	-1.41317058	2.89745939	0.00000000
C	-1.18619579	0.84607360	0.00000000
N	1.36909707	0.11559201	0.00000000
C	3.54060213	-0.36751790	0.00000000
O	-2.87592751	-0.64279456	0.00000000

E = -206.6870434 au

ZPVE = 16.3197 kcal mol⁻¹

CO ($C_{\infty v}$)

C	0.00000000	0.00000000	1.21884345
O	0.00000000	0.00000000	-0.91442322

E = -113.3033509 au

ZPVE = 3.1077 kcal mol⁻¹

HCN ($C_{\infty v}$)

C	0.00000000	0.00000000	1.05526094
N	0.00000000	0.00000000	-1.12518058
H	0.00000000	0.00000000	3.06884190

E = -93.4140816 au

ZPVE = 10.0425 kcal mol⁻¹

HNC ($C_{\infty v}$)

C	0.00000000	0.00000000	-1.29812527
N	0.00000000	0.00000000	0.91147174
H	0.00000000	0.00000000	2.79224749

E = -93.3900858 au

ZPVE = 9.7636 kcal mol⁻¹

cis-Isocyanohydroxycarbene (C_s)

H	-2.10807578	2.25988179	0.00000000
O	-2.80673214	0.55843030	0.00000000
C	-1.08849149	-1.20033306	0.00000000
N	1.30300676	-0.09997791	0.00000000
C	3.48615087	0.38286537	0.00000000

E = -206.6134087 au

ZPVE = 15.8957 kcal/mol

trans-Isocyanohydroxycarbene (C_s)

H	-4.34985021	0.09867987	0.00000000
O	-2.70153359	-0.67507993	0.00000000
C	-1.05849722	1.17014833	0.00000000
N	1.30741342	0.07090965	0.00000000
C	3.49907057	-0.36136160	0.00000000

E = -206.6179297 au

ZPVE = 16.2764 kcal/mol

TS₁ (C_s)

H	-3.50003075	1.54107779	0.00000000
O	-3.01854981	-0.66619079	0.00000000
C	-1.21147702	0.98276549	0.00000000
C	1.38988883	0.11195427	0.00000000
N	3.54693001	-0.28808739	0.00000000

E = -206.5750968 au

ZPVE = 12.6016 kcal mol⁻¹

TS₂ (C_1)

H	-3.54876827	-1.30452139	1.43989635
O	-2.94135977	-0.60606844	-0.12360752
C	-1.19587430	1.21794663	0.05110300
C	1.34205024	0.12083480	-0.01445455
N	3.48989263	-0.36110892	0.00615199

E = -206.5897702 au

ZPVE = 14.2633 kcal mol⁻¹

TS₃ (*C*₁)

H	-0.92208440	0.50669218	-2.87764592
C	-0.96808014	0.19180419	-0.85062596
C	2.11092866	1.16063107	0.35125620
N	2.12461331	-1.06311463	0.03276437
O	-2.65934523	-0.11584978	0.52728002

E = -206.6360269 au

ZPVE = 15.0774 kcal mol⁻¹

TS₄ (*C*₁)

H	-1.17076386	1.58110337	0.00000000
O	-3.04004171	0.65863530	0.00000000
C	-1.83978131	-1.32124539	0.00000000
C	1.59394867	0.35724927	0.00000000
N	3.76739597	-0.04001532	0.00000000

E = -206.5528492 au

ZPVE = 11.4827 kcal mol⁻¹

TS₅ (*C*₁)

H	-1.70967664	1.71111317	-1.34088491
O	-2.53906093	0.38367378	-0.36859822
C	-1.02565534	-1.04330877	0.79121857
C	2.28807685	-0.80647786	-0.76406276
N	1.94143513	1.02378289	0.49426324

E = -206.5594595 au

ZPVE = 14.3623 kcal mol⁻¹

TS₁₀ (*C*₁)

H	-4.11601872	-0.13226460	0.02645991
O	-2.42986816	0.38347317	-0.47369567
C	-0.88366032	-0.87336224	0.89869160
C	2.23614775	-0.89531158	-0.66599001
N	1.91271655	1.08717306	0.33975653

E = -206.5546621 au

ZPVE = 14.6353 kcal mol⁻¹

TS₁₃ (*C*_s)

H	-3.31804954	1.62115844	0.00000000
O	-2.88336304	-0.63650889	0.00000000
C	-1.06472728	0.95925685	0.00000000
N	1.37343078	0.03408074	0.00000000
C	3.58396947	-0.28677134	0.00000000

E = -206.5570747 au

ZPVE = 12.3052 kcal/mol

TS₁₄ (*C*_s)

H	-1.11459042	1.71990494	0.00000000
O	-2.81041779	0.58656286	0.00000000
C	-1.58306017	-1.36499448	0.00000000
C	3.63556369	-0.22550233	0.00000000
N	1.53149676	0.56920184	0.00000000

E = -206.5571207 au

ZPVE = 11.8484 kcal/mol

triplet Cyanohydroxycarbene **37** (*C*₁)

H	-4.31004528	0.16186163	1.19845809
O	-3.16305046	-0.47779147	-0.06173983
C	-1.04390229	0.85374115	-0.05812965
C	1.41797178	0.10722386	0.01393288
N	3.60261323	-0.28939892	0.02214146

E = -206.5999591 au

ZPVE = 15.3599 kcal mol⁻¹

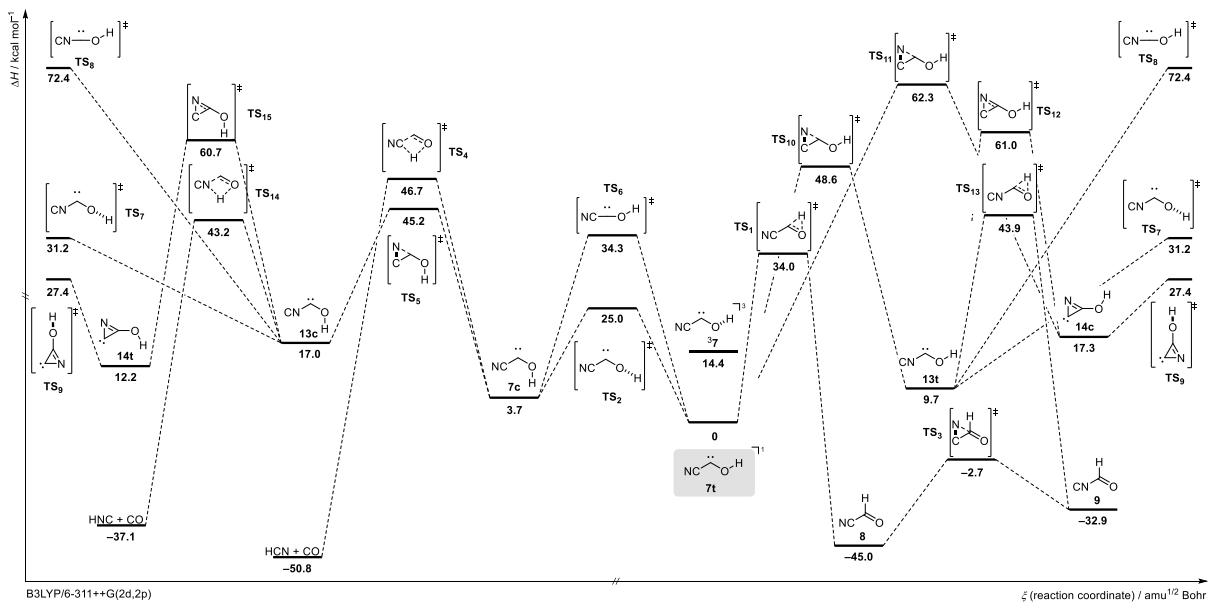


Figure S46: Extended potential energy surface (PES) around cyanohydroxycarbene **7t** including the zero-point vibrational energy (ZPVE) at B3LYP/6-311++G(2d,2p) level of theory. Note, that the PES is cyclic (left and right structures are the same).

B3LYP/6-311++G(2d,2p) optimized structures (distances in Å), electronic energies and zero-point vibrational energies (ZPVE).

trans-Cyanohydroxycarbene **7t** (C_s)

C	0.004006	0.744248	0.000000
C	0.638424	-0.546529	0.000000
N	-0.275436	1.868107	0.000000
O	-0.260493	-1.493415	0.000000
H	0.197747	-2.345801	0.000000

$$E = -206.7328612 \text{ au}$$

$$\text{ZPVE} = 16.5510 \text{ kcal mol}^{-1}$$

cis-Cyanohydroxycarbene **7c** (C_s)

C	0.032122	0.798248	0.000000
C	0.617801	-0.518948	0.000000
N	-0.245573	1.923352	0.000000
O	-0.249798	-1.489086	0.000000
H	-1.189047	-1.219420	0.000000

$$E = -206.7263931 \text{ au}$$

$$\text{ZPVE} = 16.1475 \text{ kcal mol}^{-1}$$

triplet Cyanohydroxycarbene **37** (C_s)

C	0.013859	0.790356	0.000000
C	0.377756	-0.492435	0.000000
N	-0.157073	1.960723	0.000000
O	-0.272063	-1.643896	0.000000

H 0.341768 -2.388138 0.000000

E = -206.7076895 au

ZPVE = 15.1379 kcal mol⁻¹

Cyanoformaldehyde **8** (C_s)

C	0.723419	0.083428	0.000000
C	-0.697735	0.463186	0.000000
N	1.846464	-0.169605	0.000000
O	-1.580972	-0.348625	0.000000
H	-0.876196	1.548441	0.000000

E = -206.8045415 au

ZPVE = 16.5293 kcal mol⁻¹

Isocyanoformaldehyde **9** (C_s)

C	0.462717	-0.639856	0.000000
C	-0.295606	1.824327	0.000000
N	0.000360	0.688734	0.000000
O	-0.267141	-1.581324	0.000000
H	1.556883	-0.694329	0.000000

E = -206.7847552 au

ZPVE = 16.1746 kcal mol⁻¹

HCN ($C_{\infty v}$)

C	0.000000	0.000000	-0.497085
N	0.000000	0.000000	0.649269
H	0.000000	0.000000	-1.562378

E = -93.4567975 au

ZPVE = 10.2022 kcal mol⁻¹

HNC ($C_{\infty v}$)

C	0.000000	0.000000	-0.736683
N	0.000000	0.000000	0.427922
H	0.000000	0.000000	1.424644

E = -93.4340085 au

ZPVE = 9.6176 kcal mol⁻¹

CO ($C_{\infty v}$)

C	-3.288057	1.746685	0.000000
O	-2.516083	2.565935	0.000000

E = -113.3520117 au

ZPVE = 3.1606 kcal mol⁻¹

trans-Isocyanohydroxycarbene **13t** (C_s)

C	-1.861824	-0.127112	0.000000
C	0.566330	0.562543	0.000000
N	-0.689804	0.014764	0.000000
O	1.434993	-0.418953	0.000000
H	2.316188	-0.023247	0.000000

E = -206.7167823 au

ZPVE = 16.1805 kcal mol⁻¹

cis Isocyanohydroxycarbene **13c** (C_s)

C	-0.159933	1.949286	0.000000
C	0.596788	-0.473661	0.000000
N	0.020197	0.781311	0.000000
O	-0.310881	-1.407288	0.000000
H	-1.232341	-1.078191	0.000000

E = -206.7120533 au

ZPVE = 15.7182 kcal mol⁻¹

trans-Azahydroxycyclopropylidene **14t** (C_s)

C	-1.098217	-0.746486	0.000000
C	0.144217	-0.108546	0.000000
N	-0.902479	0.647570	0.000000
O	1.444679	-0.029037	0.000000
H	1.725064	0.900733	0.000000

E = -206.7054670 au

ZPVE = 16.6331 kcal mol⁻¹

cis-Azahydroxycyclopropylidene **14c** (C_s)

C	-1.227945	-0.737155	0.000000
C	0.037321	-0.140436	0.000000
N	-0.983193	0.646590	0.000000
O	1.337365	-0.022954	0.000000
H	1.748759	-0.898720	0.000000

E = -206.7061003 au

ZPVE = 16.7269 kcal mol⁻¹

TS₁ (*C_s*)

C	0.737178	0.035091	0.000000
C	-0.624923	0.499816	0.000000
N	1.880277	-0.137832	0.000000
O	-1.615520	-0.329566	0.000000
H	-1.827882	0.847841	0.000000

E = -206.6724337 au

ZPVE = 12.5980 kcal mol⁻¹

TS₂ (*C₁*)

C	-0.004132	0.793274	0.018004
C	0.634825	-0.502072	0.022509
N	-0.258579	1.926483	0.018467
O	-0.246302	-1.505441	-0.055783
H	-0.491495	-1.848666	-0.922395

E = -206.6893791 au

ZPVE = 14.2429 kcal mol⁻¹

TS₃ (*C₁*)

C	1.148455	-0.474922	-0.359005
C	-0.606511	-0.318860	0.246725
N	1.082495	0.429280	0.398461
O	-1.407428	0.230316	-0.390841
H	-0.699940	-1.029468	1.064260

E = -206.7347279 au

ZPVE = 15.0617 kcal mol⁻¹

TS₄ (*C_s*)

C	0.865235	-0.286469	0.000000
C	-0.940072	0.676759	0.000000
N	2.001336	-0.035902	0.000000
O	-1.595959	-0.353533	0.000000
H	-0.639197	-0.902717	0.000000

E = -206.6503951 au

ZPVE = 11.4969 kcal mol⁻¹

TS₅ (*C₁*)

C	1.260336	0.372423	0.445102
C	-0.540927	0.627974	-0.359195
N	1.060139	-0.503071	-0.323745
O	-1.348985	-0.188795	0.146773
H	-0.945553	-0.970527	0.576589

E = -206.6571673 au

ZPVE = 14.2390 kcal mol⁻¹

TS₆ (*C*_s)

C	0.773553	0.000164	0.000000
C	-0.512789	-0.016305	0.000000
N	1.972976	0.011142	0.000000
O	-1.785019	-0.050694	0.000000
H	-2.188545	0.841940	0.000000

E = -206.6760683 au

ZPVE = 15.2223 kcal mol⁻¹

TS₇ (*C*₁)

C	-0.178958	1.946590	-0.017950
C	0.609902	-0.453970	-0.021427
N	-0.001685	0.774385	-0.012337
O	-0.312067	-1.424872	0.045578
H	-0.556998	-1.728351	0.928265

E = -206.6791576 au

ZPVE = 14.0181 kcal mol⁻¹

TS₈ (*C*_s)

C	1.180333	1.834143	0.000000
C	0.469710	-0.523746	0.000000
N	0.825060	0.654857	0.000000
O	0.060510	-1.733461	0.000000
H	0.794722	-2.390747	0.000000

E = -206.6140325 au

ZPVE = 14.4337 kcal mol⁻¹

TS₉ (*C*₁)

C	-1.369523	-0.209140	-0.027868
C	-0.026554	0.137798	0.036003
N	-0.263260	-1.120821	-0.007911
O	1.016665	0.962969	0.012304
H	1.323426	1.187894	0.898398

E = -206.6878332 au

ZPVE = 15.6594 kcal mol⁻¹

TS₁₀ (*C*₁)

C	1.252003	-0.465112	-0.352872
C	-0.452856	-0.474486	0.462194

N	1.066178	0.568795	0.188385
O	-1.261319	0.213680	-0.245447
H	-2.167578	-0.053414	-0.011057

E = -206.6522211 au
ZPVE = 14.5061 kcal mol⁻¹

TS₁₁ (*C*₁)

C	-1.102613	-0.116380	-0.065871
C	0.403867	-0.213978	-0.203836
N	-0.836027	-1.276759	0.142408
O	0.908921	0.963447	0.090685
H	1.873207	0.889103	0.036614

E = -206.6303515 au
ZPVE = 14.4882 kcal mol⁻¹

TS₁₂ (*C*_s)

C	0.832875	-0.769261	0.000000
C	-0.255369	0.490514	0.000000
N	1.250082	0.383853	0.000000
O	-1.395615	-0.159165	0.000000
H	-2.095905	0.511676	0.000000

E = -206.6324820 au
ZPVE = 14.5845 kcal mol⁻¹

TS₁₃ (*C*_s)

C	-0.130353	1.934726	0.000000
C	0.376056	-0.540866	0.000000
N	-0.077367	0.755388	0.000000
O	-0.473387	-1.497281	0.000000
H	0.718146	-1.743416	0.000000

E = -206.6559227 au
ZPVE = 12.2153 kcal mol⁻¹

TS₁₄ (*C*_s)

C	-1.993612	0.041017	0.000000
C	0.776968	0.761939	0.000000
N	-0.868488	-0.334099	0.000000
O	1.441293	-0.257103	0.000000
H	0.572328	-0.901827	0.000000

E = -206.6564433 au
ZPVE = 11.7985 kcal mol⁻¹

TS₁₅ (*C₁*)

C	0.820000	0.193521	-0.022866
C	-0.440062	0.009125	-0.002279
N	1.985945	-0.082519	0.020049
O -	1.705240	-0.169335	-0.007212
H	-2.299799	0.598056	0.010883

E = -206.6645892 au

ZPVE = 14.8168 kcal mol⁻¹

Full Citations for Electronic Structure Codes

Cfour:

Coupled-Cluster techniques for Computational Chemistry, a quantum-chemical program package by Stanton, J.F.; Gauss, J.; Harding, M.E.; Szalay, P.G. with contributions from Auer, A.A.; Bartlett, R.J.; Benedikt, U.; Berger, C.; Bernholdt, D.E.; Bomble, Y.J.; Christiansen, O.; Heckert, M.; Heun, O.; Huber, C.; Jagau, T.-C.; Jonsson, D.; Jusélius, J.; Klein, K.; Lauderdale, W.J.; Matthews, D.A.; Metzroth, T.; O'Neill, D.P.; Price, D.R.; Prochnow, E.; Ruud, K.; Schiffmann, F.; Stopkowicz, S.; Tajti, A.; Vázquez, J.; Wang, F.; Watts, J.D. and the integral packages MOLECULE (Almlöf, J. and Taylor, P.R.), PROPS (Taylor, P.R.), ABACUS (Helgaker, T.; Jensen, H.J. Aa.; Jørgensen, P. and Olsen, J.), and ECP routines by Mitin, A. V. and van Wüllen, C. For the current version, see; CFOUR, **2010**.

Gaussian 16:

Gaussian 16, Revision A.03; Frisch, M. J.; Trucks, G. W.; Schlegel, H. B.; Scuseria, G. E.; Robb, M. A.; Cheeseman, J. R.; Scalmani, G.; Barone, V.; Petersson, G. A.; Nakatsuji, H.; Li, X.; Caricato, M.; Marenich, A. V.; Bloino, J.; Janesko, B. G.; Gomperts, R.; Mennucci, B.; Hratchian, H. P.; Ortiz, J. V.; Izmaylov, A. F.; Sonnenberg, J. L.; Williams-Young, D.; Ding, F.; Lipparini, F.; Egidi, F.; Goings, J.; Peng, B.; Petrone, A.; Henderson, T.; Ranasinghe, D.; Zakrzewski, V. G.; Gao, J.; Rega, N.; Zheng, G.; Liang, W.; Hada, M.; Ehara, M.; Toyota, K.; Fukuda, R.; Hasegawa, J.; Ishida, M.; Nakajima, T.; Honda, Y.; Kitao, O.; Nakai, H.; Vreven, T.; Throssell, K.; Montgomery, J. A., Jr.; Peralta, J. E.; Ogliaro, F.; Bearpark, M. J.; Heyd, J. J.; Brothers, E. N.; Kudin, K. N.; Staroverov, V. N.; Keith, T. A.; Kobayashi, R.; Normand, J.; Raghavachari, K.; Rendell, A. P.; Burant, J. C.; Iyengar, S. S.; Tomasi, J.; Cossi, M.; Millam, J. M.; Klene, M.; Adamo, C.; Cammi, R.; Ochterski, J. W.; Martin, R. L.; Morokuma, K.; Farkas, O.; Foresman, J. B.; Fox, D. J., Gaussian Inc., Wallingford CT **2016**.

NBO6:

NBO 6.0. E. D. Glendening, J. K. Badenhoop, A. E. Reed, J. E. Carpenter, J. A. Bohmann, C. M. Morales, C. R. Landis, and F. Weinhold, Theoretical Chemistry Institute, University of Wisconsin, Madison **2013**.

Polyrate 2017-C:

POLYRATE 2017-C; Zheng, J.; Bao, J. L.; Meana-Pañeda, R.; Zhang, S.; Lynch, B. J.; Corchado, J. C.; Chuang, Y.-Y.; Fast, P. L.; Hu, W.-P.; Liu, Y.-P.; Lynch, G. C.; Nguyen, K. A.; Jackels, C. F.; Ramos, A. F.; Ellingson, B. A.; Melissas, V. S.; Vill, J.; Rossi, I.; Coitio, E. L.; Pu, J.; Albu, T. V.; Steckler, R.; Garrett, B. C.; Isaacson, A. D.; Truhlar, D. G., 2017.

ChemShell:

ChemShell, a Computational Chemistry Shell, see www.chemshell.org

CYLview:

CYLview, 1.0b; Legault, C. Y., Université de Sherbrooke, 2009 (<http://www.cylview.org>)

References

- (1) Čížek, J. *J. Chem. Phys.* **1966**, *45*, 4256-4266.
- (2) Bartlett, R. J.; Watts, J. D.; Kucharski, S. A.; Noga, J. *Chem. Phys. Lett.* **1990**, *165*, 513-522.
- (3) Raghavachari, K. *Annu. Rev. Phys. Chem.* **1991**, *42*, 615-642.
- (4) Stanton, J. F. *Chem. Phys. Lett.* **1997**, *281*, 130-134.
- (5) Dunning, J., Thom H. *J. Chem. Phys.* **1989**, *90*, 1007-1023.
- (6) Becke, A. D. *Phys. Rev. A* **1988**, *38*, 3098-3100.
- (7) Becke, A. D. *J. Chem. Phys.* **1993**, *98*, 5648-5652.
- (8) Lee, C.; Yang, W.; Parr, R. G. *Phys. Rev. B* **1988**, *37*, 785-789.
- (9) Vosko, S. H.; Wilk, L.; Nusair, M. *Can. J. Phys.* **1980**, *58*, 1200-1211.
- (10) Møller, C.; Plesset, M. S. *Phys. Rev.* **1934**, *46*, 618-622.
- (11) Hratchian, H. P.; Schlegel, H. B. *J. Phys. Chem. A* **2002**, *106*, 165-169.
- (12) Hratchian, H. P.; Schlegel, H. B. *J. Chem. Phys.* **2004**, *120*, 9918-9924.
- (13) Mathematica 10.3; Wolfram Research, I., Champaign, Illinois **2015**.
- (14) Kuppermann, A.; Truhlar, D. G. *J. Am. Chem. Soc.* **1971**, *93*, 1840-1851.
- (15) Skodje, R. T.; Truhlar, D. G.; Garrett, B. C. *J. Phys. Chem.* **1981**, *85*, 3019-3023.
- (16) Rommel, J. B.; Goumans, T. P. M.; Kästner, J. *J. Chem. Theory Comput.* **2011**, *7*, 690-698.
- (17) Kästner, J.; Carr, J. M.; Keal, T. W.; Thiel, W.; Wander, A.; Sherwood, P. *J. Phys. Chem. A* **2009**, *113*, 11856-11865.
- (18) Skell, P. S.; Wescott, L. D.; Golstein, J. P.; Engel, R. R. *J. Am. Chem. Soc.* **1965**, *87*, 2829-2835.
- (19) Ireland, C. J.; Jones, K.; Pizey, J. S.; Johnson, S. *Synth. Commun.* **1976**, *6*, 185-191.
- (20) Yamada, Y.; Yasuda, H. *Synthesis* **1990**, *1990*, 768-770.
- (21) Linn, W. J.; Webster, O. W.; Benson, R. E. *J. Am. Chem. Soc.* **1965**, *87*, 3651-3656.
- (22) Achmatowicz, O.; Szymoniak, J. *Tetrahedron* **1982**, *38*, 1299-1302.